

بِسْمِ اللَّهِ الرَّحْمَنِ الرَّحِيمِ



Organisation of Islamic Cooperation

## **Improvement of heat transfer in helical HX with multiple-head ribbed using water-based nanofluids**

A thesis submitted to the department of Mechanical and Production Engineering (MPE), Islamic University of Technology (IUT), in the fulfillment of the requirement for degree of Bachelor in Mechanical Engineering.

**Prepared By:**

**Md. Jahid Hasan (160011021)**

**Supervised By: Dr. Arafat Ahmed Bhuiyan**

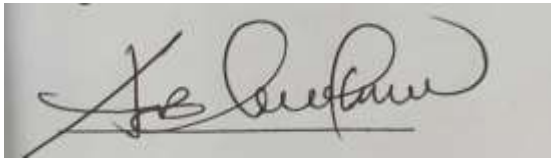
**Department of Mechanical and Production Engineering**

**Islamic University of Technology**

## **CERTIFICATE OF RESEARCH:**

The thesis title “**Improvement of heat transfer in helical tube HX with multiple-head ribbed using water-based nanofluids**” submitted by **MD. JAHID HASAN (160011021)**, has been accepted as satisfactory in fulfillment of the requirement for the Degree of Bachelor of science in Mechanical and Production Engineering on March, 2021.

Signature of the Supervisor

A handwritten signature in black ink on a light-colored background. The signature is cursive and appears to read 'Dr. Arafat Ahmed Bhuiyan'.

---

Dr. Arafat Ahmed Bhuiyan

Department of Mechanical and Production Engineering

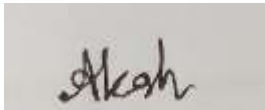
Islamic University of Technology

## **CANDIDATE DECLARATION**

---

It is hereby declared that this thesis or any part of it has not been submitted elsewhere for the award of any degree.

**Signature of the Candidate.**



---

**Md. Jahid Hasan**

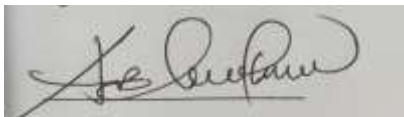
**Student ID: 160011021**

**Department of Mechanical & Production Engineering (MPE)**

**Islamic University of Technology (IUT), OIC**

**Board Bazar, Gazipur Bangladesh.**

**Signature of the Supervisor**



---

**Dr. Arafat Ahmed Bhuiyan**

**Department of Mechanical & Production Engineering (MPE)**

**Islamic University of Technology (IUT), OIC**

**Board Bazar, Gazipur Bangladesh.**

## **ACKNOWLEDGEMENT:**

I express my heartiest gratefulness to Almighty Allah for His divine blessings, which made me possible to complete this thesis successfully.

First and foremost, I feel grateful and acknowledge our profound indebtedness to Dr. Arafat Ahmed Bhuiyan, Department of Mechanical and Production Engineering, IUT. His endless patience, scholarly guidance, continual encouragement, constant and energetic supervision, constructive criticism, valuable advice at all stages has made it possible to complete this project. I would also like to offer thanks to all who helped me in many ways during the project work. I acknowledge my sincere indebtedness and gratitude to my parents for their love.

I seek excuse for any errors that might be in this report despite our best efforts.

## **ABSTRACT:**

This study shows the comparison between the helical and straight tube heat exchangers with multiple-head ribbed geometries. A computational fluid dynamics model with constant wall temperature condition was developed for the study and validated against a numerical study and particular experimental correlations. Two, three, and four head ribbed geometries were used for both the helical and straight tubes. Also, different revolutions of ribbed geometry were taken into consideration while designing the HXs for the comparison of heat transfer. Number of 10, 20, and 30 coil revolutions were used in this study. Four different water-based nanofluids, such as  $\text{Al}_2\text{O}_3$ ,  $\text{CuO}$ ,  $\text{SiO}_2$ ,  $\text{ZnO}$  used in the best heat exchanger. Results have been shown in terms of the effect of ribbed geometry, coil revolutions, velocity, and temperature distribution along the pipe and the effect of nanofluid in the heat exchanger. Helical tube heat exchangers are more effective than straight tube heat exchangers in terms of heat transfer. It was found that the lesser the number of ribbed heads, the higher the heat transfer for both helical and straight heat exchangers. On the other side, when the number of coil revolution of ribbed profile increases, the heat transfer is also increased for both helical and straight heat exchangers. So, the two head ribbed with 30 coil revolutions helical heat exchanger ensures the highest amount of heat transfer rate. And four head ribbed with 10 coil revolution straight tube heat exchanger has got the lowest value of heat transfer rate. In the nanofluid study, it is found that the  $\text{Al}_2\text{O}_3$  water-based nanofluid has the highest heat transfer rate among the four nanoparticles. Finally, this study represents the perfect comparison to choose the right type of heat exchanger and the nanoparticle.

### **Keywords**

Heat Transfer, Laminar flow, Helical heat exchanger, Multiple-head ribbed tube, Water-based Nanofluid.

## **LIST OF FIGURES:**

Figure 3.1 Schematic diagram of (a) helical heat exchanger (b) straight heat exchanger .....	08
Figure 3.2 The cross-sectional profile of (a) two-head ribbed (b) three-head ribbed (c) four-head ribbed for both helical and straight heat exchangers .....	14
Figure 3.3 Schematic diagram of helical heat exchanger .....	15
Figure 3.4 Schematic diagram of straight heat exchanger .....	16
Figure 3.5 Schematic diagram of a tube in tube helical heat exchanger for nanofluid .....	17
Figure 5.1 Validation graph of (a) Nu vs $Gz^{-1}$ plot for straight pipes (b) Nu vs $De$ plot for helical pipes .....	24
Figure 5.2 Axial velocity profile contour in helical heat exchanger .....	25
Figure 5.3 Axial velocity profile contour in straight heat exchanger .....	26
Figure 5.4 Temperature distribution contour in helical heat exchanger .....	28
Figure 5.5 Temperature distribution contour in straight heat exchanger .....	29
Figure 5.6 Nusselt number vs local distance plot of (a) helical pipes with (b) straight pipes.....	31
Figure 5.7 Nusselt number vs local distance plot of helical heat exchanger with (a) 10 revolution (b) 20 revolution (c) 30 revolution ... ..	35
Figure 5.8 Nusselt number vs local distance plot of straight pipe with (a) 10 revolution (b) 20 revolution (c) 30 revolution.....	38
Figure 5.9 Nusselt number vs local distance plot of helical pipe with (a) two-head ribbed (b) three-head ribbed (c) four-head ribbed with different revolutions .....	42
Figure 5.10 Nusselt number vs local distance plot of straight pipe with (a) two-head ribbed (b) three-head ribbed (c) four-head ribbed with different revolutions .....	45
Figure 5.11 Nusselt number vs Dean number plot for water based nanofluids.....	46
Figure 5.12 Temperature distribution of tube in tube heat exchanger.....	47

**LIST OF TABLES:**

Table 3.1 Thermophysical properties of various water-based nanofluids .....12

Table 3.2 All the geometric cases both for helical and straight heat exchangers .....13

Table 4.1 Geometrical parameters and fluid properties used in this study .....19

Table 4.2 Different inlet velocity of water at the outer pipe for nanofluid study .....21

**CONTENTS:**

*Chapter 1* *1-2*

---

**INTRODUCTION**

*Chapter 2* *3-6*

---

**LITERATURE REVIEW**

*Chapter 3* *7-17*

---

**GEOMETRY AND MATHEMATICAL FORMULATION**

*Chapter 4* *18-21*

---

**NEUMERICAL METHODOLOGY**

*Chapter 5* *22-47*

---

**RESULTS AND DISCUSSIONS**

*Chapter 6* *48*

---

**CONCLUSIONS**





# ***CHAPTER 1:***

## ***INTRODUCTION***

A heat exchanger is a system used to transfer heat between two or more fluids. Heat exchangers are used in both cooling and heating processes. The fluids may be separated by a solid wall to prevent mixing or they may be in direct contact. Heat exchangers, metal shells and tubes, work by transferring heat from one place to another. When a furnace burns natural gas or propane fuel, its exhaust/combustion by-products (also known as flue gas) enter and travel through the heat exchanger. The hot flue gas heats the metal as the gas makes its way to the exhaust outlet of the furnace. As this is happening, the hot metal heats the air circulating over the exterior of the heat exchanger. Heat exchanger is used in almost every industrial application while designing a component. It is used including refrigeration, air conditioning, powerplants, space applications, etc. There are many types of heat exchangers available and people used the particular heat exchanger for particular cases or applications. Among them, helical heat exchangers or coil-type heat exchangers are used from a very early stage. Due to the shape, there is an effect of centrifugal force in the helical heat exchanger. It has a better heat transfer performance than the straight pipes due to the curvature which generates the secondary flow to help the better fluid mixing. Nanofluid is a colloidal suspension of nanoparticles on a base fluid such as water, Ethylene glycol, engine oil, etc. Nanofluids are used to enhance the better heat transfer in almost many applications such as nuclear reactors, fuel cells, thermal cooling, etc. The thermal conductivity of nanoparticles is higher than the base fluid. So, mixing the nanoparticles at a certain concentration in the base fluid excessively increase the thermal conductivity of the fluid.

The present study introduces new design considerations to compare the effect of the geometrical shape of HX by applying rib in the geometry with various coil revolutions. Both the helical and the straight pipes are analyzed by changing the cross sections using multiple ribs. 18 different geometries are compared in terms of heat transfer effect. Local Nusselt number is plotted for all the geometries. Finally, this study is incorporated with an inner tube using four different water based nanofluids to show the heat transfer effect on the most effective heat exchanger among the 18 HXs.

## ***CHAPTER 2:***

### ***LITERATURE REVIEW***

Kurnia et al. [1] numerically investigated the heat transfer effect and entropy generation of helical tubes with three different cross-sections. They also compared the straight and helical pipe flow. They found a coiled tube with square cross-section yields the highest heat transfer performance. Also, square cross-section generates the highest entropy compared to the ellipse and circular.

Gord et al. [2] worked on the tube in tube helical heat exchanger and found the heat transfer effect by varying dean number, Prandtl number, the ratio of the helical pipe diameter to the tube diameter, duty parameter. Combining economic analysis with an entropy generation minimization analysis also carried out in this study for future work in this context to promote application of double-pipe helical heat exchangers.

Srinivas and Vinod [3] experimented with Al<sub>2</sub>O<sub>3</sub> nanofluid in the helical coil heat exchanger. The comparison has been made when nanofluid and base fluid (water) are used as heating medium. They proved that the maximum energy savings could be possible 10.65%. They also observed that, energy savings are more in laminar and turbulent conditions of flow than transition regime, and percentage savings increase with increase in nanoparticle concentration. Higher stirrer speed and shell-side fluid temperature also resulted in more energy savings.

Narrein and Mohammed [4] worked on four different nanofluids ( $\text{Al}_2\text{O}_3$ ,  $\text{SiO}_2$ ,  $\text{CuO}$ ,  $\text{ZnO}$ ) in a helically coiled tube heat exchanger with rotation and used water, ethylene glycol, engine oil as base fluids. They found that the Nusselt number is highest using  $\text{CuO}$ -water nanofluid in this study. In addition, rotation can be used to enhance the heat transfer rates.

M.A. Khairul et al. [5] numerically experimented on water-based nanofluid in a helically coiled heat exchanger without rotation. They concluded that the heat transfer coefficient increases with the increase of volume concentration of nanofluid.  $\text{CuO}$ /water nanofluids could increase the heat transfer coefficient and decrease the entropy generation about 7.14% and 6.14% respectively. For equal volume flow rate, mass flow rate could be increased by injecting nanoparticles in base fluid only and represented higher efficiency.

Srinivas and Vinod [6] worked on the shell and helical heat exchanger with three different water-based nanofluids. They found that higher values of nanofluid concentration, stirrer speed, and shell-side fluid temperature resulted in greater effectiveness of heat exchanger. A maximum increase of 30.37%, 32.7% and 26.8% in effectiveness of heat exchanger they observed for  $\text{Al}_2\text{O}_3$ ,  $\text{CuO}$  and  $\text{TiO}_2$ /water nanofluids respectively, when compared to water, indicating intensification of heat transfer.

Kannadasan et al. [7] experimentally worked on  $\text{CuO}$  water-based nanofluids in the horizontal and vertical helical heat exchanger with different volume concentrations. They showed that there are no significant differences in convective heat transfer coefficients in setting up the horizontal

and vertical helical heat exchanger. Also, they concluded that the friction factor goes higher when the volume concentration is higher and the flow rate is low.

Seara et al. [8] numerically evaluated the performance of a vertical helical coil heat exchanger. They found that the larger the pipe diameter larger the Nusselt number and also the larger the heat transfer rate to pressure drop ratio. Gnanavel et al. [9] worked on spiral spring which is placed in a double tube heat exchanger using four different nanofluids, and found that the higher the Reynolds number higher the Nusselt number. They also analyzed the friction factor of using different nanofluids.

Huminic and Huminic [10] had investigated the heat transfer rate of a double-tube helical heat exchanger using two nanofluids CuO and TiO<sub>2</sub> with 0.5-3vol.% concentrations. They found that the heat transfer rate of the nanofluid is 19% greater than the pure water while nanofluid is used in the inner pipe.

Kumar et al. [11] experimentally and numerically studied the pressure drop and heat transfer effect of a tube in a tube helical heat exchanger. They observed that the heat transfer rate increases when the inner tube dean number increases. In the variation of overall heat transfer coefficient, they observed for different flow rates in the annulus region for a constant flow rate in the inner-coiled tube.

An experimental work of heat transport capability in a nanofluid oscillating heat pipe was carried out by Ma et al. [12] They used 1.0vol % diamond in the HPLC grade water of 5-50nm. They

noticed that the operating temperature has a significant effect on the heat transfer rate. They also observed that OHP charged with nanofluids can reach a thermal resistance of  $0.03^{\circ}\text{C}/\text{W}$  at a power input of 336 W.

Rennie et al. [13] experimentally evaluated the heat transfer characteristics of a double pipe helical heat exchanger for both parallel flow and counterflow. They observed that the heat transfer rate was higher in the counter flow as there are larger temperature differences. They also showed the overall heat transfer rate and the dean number effect in the pipe.

Shafahi et al. [14] numerically investigated thermal performance in a two-dimensional heat pipe using three different nanofluids  $\text{Al}_2\text{O}_3$ ,  $\text{CuO}$ , and  $\text{TiO}_2$ . They found that the nanoparticles within the liquid enhance the thermal performance of the heat pipe by reducing the thermal resistance while enhancing the maximum heat load it can carry. They also reported smaller the nanoparticles higher the temperature gradient along the heat pipe.

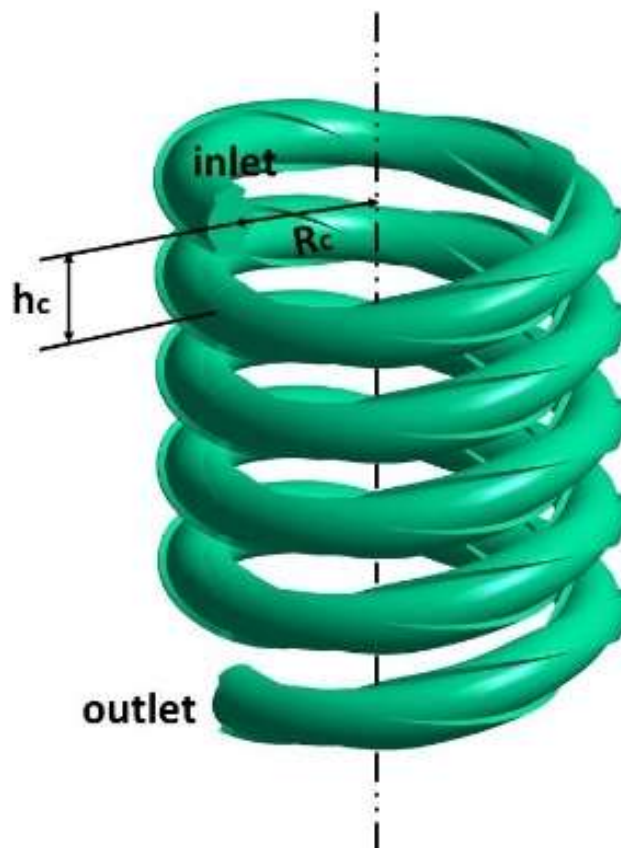
Wu et al. [15] experimentally investigated the pressure drop of double pipe helical heat exchanger using five different concentration alumina nanofluids. They that the heat transfer enhancement of the nanofluids compared to water is from 0.37% to 3.43% according to the constant flow velocity basis.

Xu et al. [16] introduced the ribbed geometry profile in a straight pipe. They used four head ribbed tube to investigate the thermal performance using Therminol. Experimentally they showed that the ribbed geometry tube is 1.05-1.35 times higher than the plain tube.

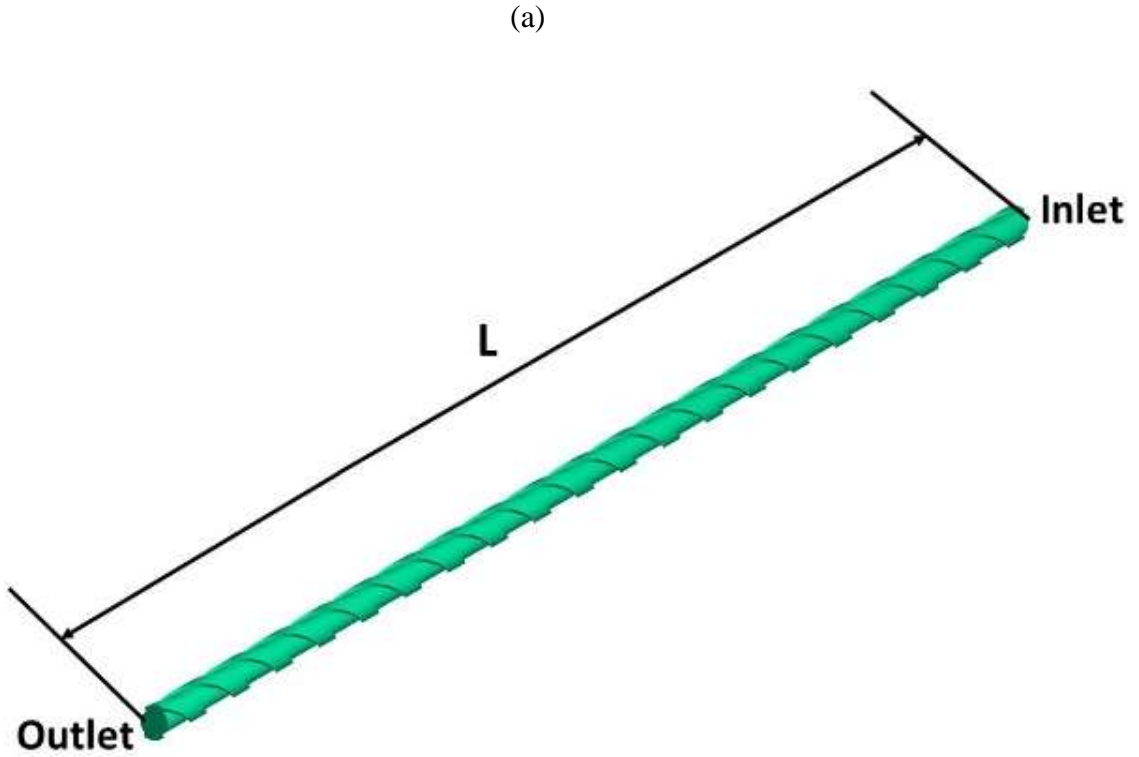
## **CHAPTER 3:**

### **GEOMETRY AND MATHEMATICAL FORMULATIONS**

A computational fluid dynamics study was carried out with the same constant wall temperature condition and a large temperature difference between fluid and the wall. All the geometrical parameters and the fluid properties are given in [Table 4.1](#) to design the heat exchanger. Thermophysical properties of nanofluids are placed in [Table 3.1](#). For all the cases, governing equations and the mathematical equations will be discussed step by step in this chapter.







(b)

**Figure 3.1** Schematic diagram of (a) helical heat exchanger (b) straight heat exchanger

### 3.1. Governing equations

To solve the 3D computational fluid dynamics model the Reynolds Averaged Navier-Stokes (RANS) equations were used considering the flow field as laminar. The governing equations are

as follows,

Continuity equations:

$$\frac{\partial(\rho u_i)}{\partial x_i} = 0 \tag{1}$$

Momentum equations:

$$\frac{\partial(\rho u_i)}{\partial t} + \frac{\partial(\rho u_i u_j)}{\partial x_j} = - \frac{\partial p}{\partial x_i} + \frac{\partial}{\partial x_j} \left( \mu \frac{\partial u_i}{\partial x_j} \right) - \overline{\rho u'_i u'_j} \tag{2}$$

Energy

equations:

$$\frac{\partial}{\partial x_i}(\rho T) + \frac{\partial}{\partial x_i}(\rho u_i T) = \frac{\partial}{\partial x_i} \left( \frac{\gamma}{c_p} \frac{\partial T}{\partial x_i} \right) \quad (3)$$

where,  $\rho$  is the density of fluid,  $T$  = temperature,  $u_i$  = inlet velocity,  $C_p$  = specific heat

### 3.2. Used mathematical equations

Due to high wall temperature, water is not used as fluid for analyzing the geometrical effect of the HXs. So, for all the cases, except the nanofluid part, air is considered as material for the study. As there will be temperature variations across the pipe all the physical properties of air will not be the same in all the positions. The density, dynamic viscosity, thermal conductivity, and specific gravity of air were set as polynomial functions of temperature with the following

four constitutive equations,

Density,

$$\rho = C_{\rho,1}T^2 - C_{\rho,2}T + C_{\rho,3} \quad (4)$$

Dynamic

Viscosity,

$$\mu = C_{\mu,1}T^2 + C_{\mu,2}T + C_{\mu,3} \quad (5)$$

Thermal

conductivity,

$$k = C_{k,1}T^2 + C_{k,2}T + C_{k,3} \quad (6)$$

Specific

heat,

$$c_p = C_{cp,1}T^2 + C_{cp,2}T + C_{cp,3} \quad (7)$$

the values of  $C_{\rho,1}$ ,  $C_{\rho,2}$ ,  $C_{\rho,3}$ ,  $C_{\mu,1}$ ,  $C_{\mu,2}$ ,  $C_{\mu,3}$ ,  $C_{k,1}$ ,  $C_{k,2}$ ,  $C_{k,3}$ ,  $C_{cp,1}$ ,  $C_{cp,2}$ ,  $C_{cp,3}$  are placed in [Table 4.1](#).

However, water is used as base fluid for analyzing the effect of nanofluids.

Mixed mean temperature can be calculated as,

$$T_{mean} = \frac{1}{VA_c} \int_{A_c} uT dA_c \quad (8)$$

where,  $A_c$  is the cross-sectional area of the pipe. Velocity can be calculated as,

$$V = \frac{1}{A_c} \int_{A_c} u dA_c \quad (9)$$

Nusselt Number is the ratio of convective to conductive heat transfer across a boundary. It can be calculated as,

$$Nu = \frac{hD_h}{k} \quad (10)$$

where,  $h$  is heat transfer coefficient,  $D_h$  is the hydraulic diameter of the pipe and  $k$  is the thermal conductivity of the fluid.

Heat transfer coefficient can be expressed as,

$$h = \frac{q_{wall}}{LMTD} \quad (11)$$

where,  $q_{wall}$  is the wall heat flux, LMTD is the log mean temperature difference.

As this study is considered as constant wall temperature condition, so while calculating the wall heat flux condition, LMTD should be taken into consideration while using the formula.

$$LMTD = \frac{\Delta T_1 - \Delta T_2}{\ln\left(\frac{\Delta T_1}{\Delta T_2}\right)} \quad (12)$$

where,  $\Delta T_1$  is the inlet temperature difference and  $\Delta T_2$  is the outlet temperature difference.

Convective heat transfer rate can be calculated as,

$$Q = hA_s(T_{wall} - T_{mean}) \quad (13)$$

Where,  $h$  = convective heat transfer coefficient,  $A_s$  = surface area of the pipe,

$T_{wall}$  = wall temperature,  $T_{mean}$  = mean temperature

Mass flow rate is calculated as,

$$\dot{m} = \rho A_c U_{in} \quad (14)$$

where,  $\rho$  is the density,  $A_c$  is the cross-sectional area of the pipe and  $U_{in}$  is the inlet velocity of

the fluid.

The thermophysical properties of nanofluids can be obtained from the following equations,

Density [17] :

$$\rho_{nf} = (1-\phi) \rho_{bf} + \phi \rho_{np} \quad (15)$$

Heat capacity [17] :

$$(\rho c_p)_{nf} = (1-\phi) (\rho c_p)_{bf} + \phi (\rho c_p)_{np} \quad (16)$$

Effective thermal conductivity [17]:

$$k_{eff} = k_{Static} + k_{Brownian} \quad (17)$$

Static thermal conductivity [17] :

$$k_{Static} = k_{bf} \left[ \frac{k_{np} + 2k_{bf} - 2(k_{bf} - k_{np})\phi}{k_{np} + 2k_{bf} + (k_{bf} - k_{np})\phi} \right] \quad (18)$$

Brownian thermal conductivity [17] :

$$k_{Brownian} = 5 \times 10^4 \beta \phi \rho_{bf} c_{p,bf} \sqrt{\frac{\kappa T}{2 \rho_{np} R_{np}}} \times f(T, \phi) \quad (19)$$

where Boltzmann constant is

$$\kappa = 1.3807 \times 10^{-23} \frac{J}{K} \quad (20)$$

Modeling function (CuO),  $\beta$  [18]:

$$\beta = 9.881(100\phi)^{-0.9446} \text{ for } 1\% \leq \phi \leq 6\% \quad (21)$$

Modeling function (Al<sub>2</sub>O<sub>3</sub>),  $\beta$  [18]:

$$\beta = 8.4407(100\phi)^{-1.07304} \text{ for } 1\% \leq \phi \leq 10\% \quad (22)$$

Modeling function (ZnO),  $\beta$  [18]:

$$\beta = 8.4407(100\phi)^{-1.07304} \text{ for } 1\% \leq \phi \leq 7\% \quad (23)$$

Modeling function (SiO<sub>2</sub>),  $\beta$  [19]:

$$\beta = 1.9526(100\phi)^{-1.4594} \text{ for } 1\% \leq \phi \leq 10\% \quad (24)$$

Modeling function,  $f(T, \phi)$  [19]:

$$f(T, \phi) = (2.8217 \times 10^{-2} \phi + 3.917 \times 10^{-3}) \left(\frac{T}{T_0}\right) + (-3.0699 \times 10^{-2} \phi - 3.91123 \times 10^{-3}) \quad (25)$$

Dynamic viscosity [20]:

$$\frac{\mu_{eff}}{\mu_{bf}} = \frac{1}{1 - 34.87 \left(\frac{d_{np}}{d_{bf}}\right)^{-0.3} \phi^{1.03}} \quad (26)$$

Equivalent diameter of the base fluid molecule will be [19]:

$$d_{bf} = \left[ \frac{6M}{N\pi\rho_{bf}} \right] \quad (27)$$

From above all the equations, thermophysical properties of Al<sub>2</sub>O<sub>3</sub>, CuO, SiO<sub>2</sub>, and ZnO are obtained which are shown in **Table 3.1**. Here, water is considered as base fluid for all of these particles.

**Table 3.1:** Thermophysical properties of various water-based nanofluids.

Parameters	Al <sub>2</sub> O <sub>3</sub>	CuO	SiO <sub>2</sub>	ZnO
Density (Kg/m <sup>3</sup> )	1117.075	1218.275	1046.275	1182.275
Viscosity (N s/m <sup>3</sup> )	0.0015795	0.0015795	0.0015795	0.0015795
Heat capacity (J/kg K)	3696	3404	3890	3484
Thermal conductivity (W/mK)	0.774499	0.779402	0.647057	0.753817
Thermal expansion (1/K)	0.000178	0.000189	0.000189	0.00016

### 3.3. Considered Cases

As one of the goals of this study is to observe the geometrical effect both for helical and straight heat exchangers. So, nine cases for each of the helical and the straight pipes are selected for the

analysis which is shown in [Table 3.2](#). Three different number of ribs, and also three different coil revolutions were chosen to see the effect. Case 1-3, Case 4-6, and Case 7-9 are the sets of constant rib number of the geometries to evaluate the coil revolution effect of the geometrical study.

**Table 3.2:** All the geometric cases both for helical and straight heat exchangers.

Case No	Case Names
Case 1	2 rib and 10 revolution
Case 2	2 rib and 20 revolution
Case 3	2 rib and 30 revolution
Case 4	3 rib and 10 revolution
Case 5	3 rib and 20 revolution
Case 6	3 rib and 30 revolution
Case 7	4 rib and 10 revolution
Case 8	4 rib and 20 revolution
Case 9	4 rib and 30 revolution

Schematic representations of the helical and the straight heat exchanger are shown in [Figure 3.1](#) with required notations for preparing the fluid domain of three-dimensional CFD model. All the parameters for the design are placed in [Table 4.1](#) along with the other properties. Three different cross-sectional geometries such as 2 rib, 3 rib and 4 rib profiles are chosen for this study which are shown with proper dimensions in [Figure 3.2](#). Geometry profile dimensions are slightly different from one another to keep the same hydraulic diameter ( $D_h$ ), as local Nusselt

number is observed for each of the cases.

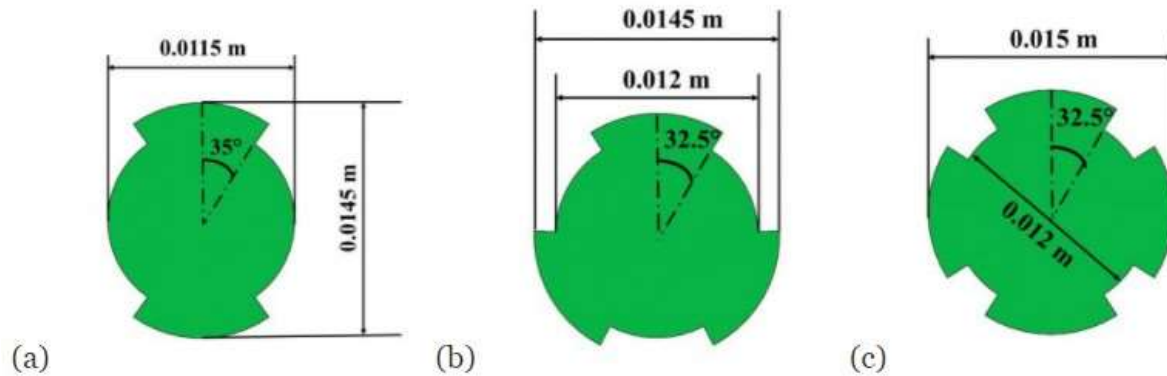


**Figure 3.2** The cross-sectional profile of (a) two-head ribbed (b) three-head ribbed (c) four-head ribbed for both helical and straight heat exchangers

Nine different 3D models of helical heat exchangers are designed considering the cases mentioned above [Table 3.1](#). Those are represented in [Figure 3.3](#). They are also being followed the overall helical heat exchanger parameters which are shown in [Figure 3.1\(a\)](#) and [Table 4.1](#). Also, the specific cross-sectional profiles of different rib geometry are represented in [Figure 3.2](#).

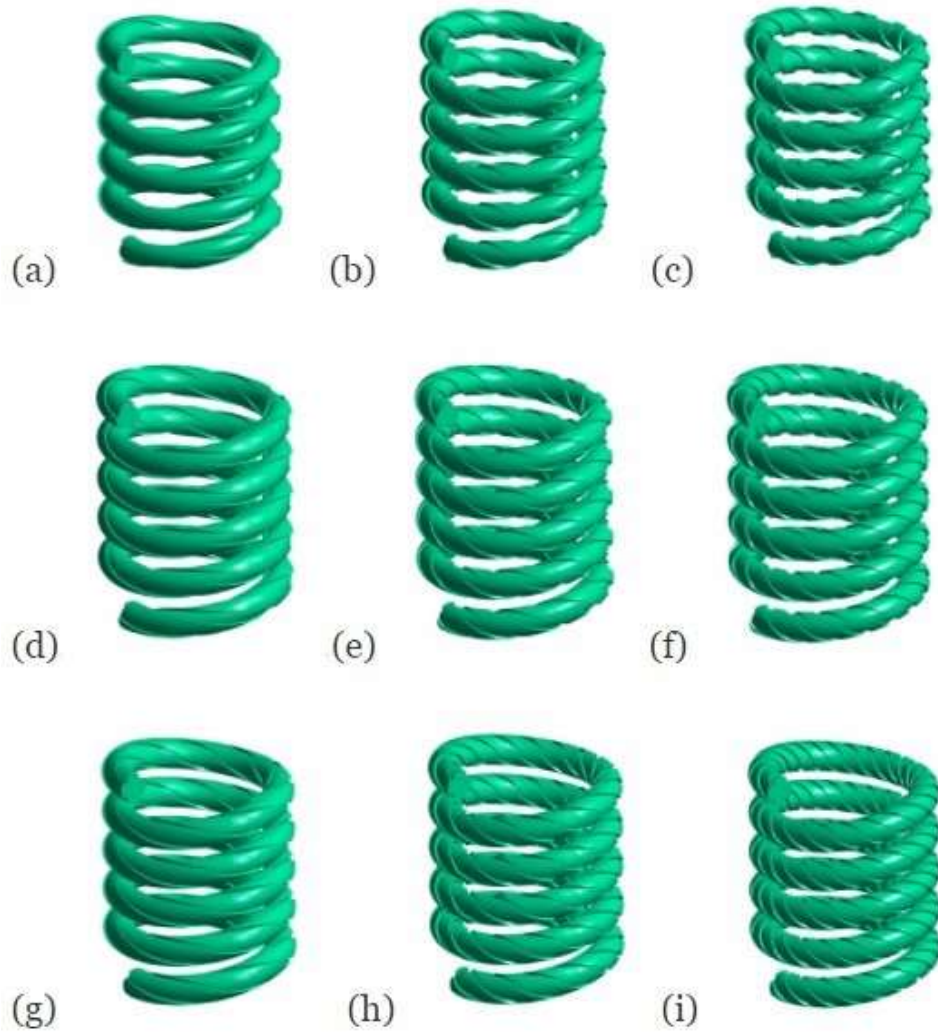


**Figure 3.3** Schematic diagram of helical heat exchanger of (a) Case 1 (b) Case 2 (c) Case 3 (d) Case 4 (e) Case 5 (f) Case 6 (g) Case 7 (h) Case 8 (i) Case 9

Also, nine different 3D models of straight heat exchangers are designed considering the cases mentioned above in [Table 3.1](#). Those are represented in [Figure 3.4](#). This design is very straightforward with parameters which are placed in [Figure 3.1\(b\)](#) and [Table 4.1](#). The specific cross-sectional profile of



different rib geometries is represented in [Figure 3.2](#).

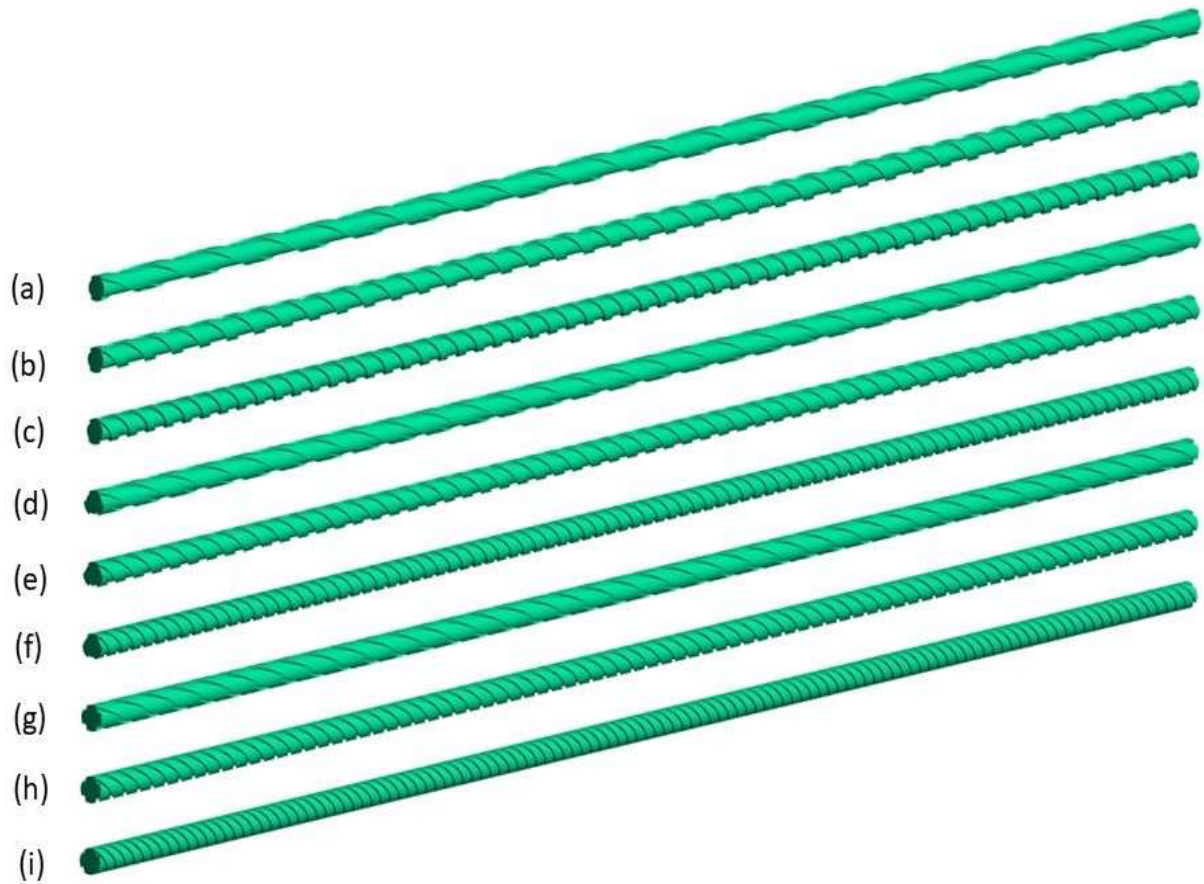


**Figure 3.4** Schematic diagram of straight heat exchanger of (a) Case 1 (b) Case 2 (c) Case 3 (d) Case 4 (e) Case 5 (f) Case 6 (g) Case 7 (h) Case 8 (i) Case 9

In the final section of the study, the effect of different water-based nanofluids is analyzed in the highest effective heat exchangers among the total of eighteen HXs. Four different water-based nanofluids were chosen for the comparative study. A tube in tube heat exchanger was designed which is shown in [Figure 3.5](#). 5mm diameter circular pipe was inserted as the nanofluid fluid domain, the outer ribbed pipe is the same dimensioned as before. Water passes through the outer

ribbed pipe and four different nanofluids pass through the inner circular tube. A thin wall was placed for the heat transfer between nanofluid pipe and the outer ribbed pipe. The boundary conditions for this analysis are described in the following chapter.

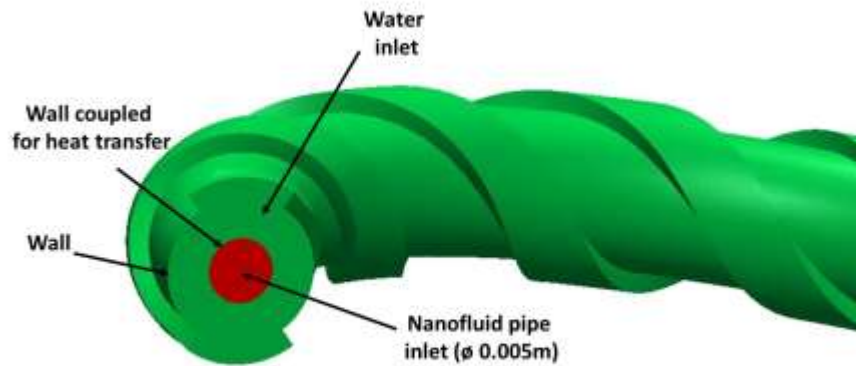


**Figure 3.5** Schematic diagram of a tube in tube helical heat exchanger for analyzing nanofluid.

## **CHAPTER 4:**

### ***NUMERICAL***

### ***METHODOLOGY***

The study was performed numerically with the help of multiple software packages and then validated against some experimental correlations and numerical simulations done by others. The numerical approach and methodology will be discussed step by step in this chapter.

#### **4.1. Solving technique**

3D CAD geometries of fluid domains of all the cases were created in SolidWorks. Origin was taken at the inlet position for all the geometries. Negative Y-axis denotes the direction of the gravitational force and positive X-axis is taken for inlet fluid flow direction. Geometries were imported to Ansys Mechanical 2019R3 for grid generation. High orthogonal quality (0.61) and low skewness values (0.26) were taken into consideration for better mesh quality. Also, near-wall treatment was applied for a good result as there were lots of curvatures. Edge sizing is applied for the sizing of the mesh through the ribbed edges. Mesh independence study was done by the Kurnia et al. [1] for a similar model of same hydraulic diameter with same dimensions. In that numerical experiment, they used  $5.6 \times 10^5$  to  $1.1 \times 10^6$  elements for meshing. In this study, the range of mesh elements were strictly maintained to get the desired heat transfer result. A steady-state simulation was performed using commercial software Ansys Fluent 2019R3 with the pressure-based coupled solver. Pressure-velocity coupling based algorithm SIMPLE was chosen for conducting the simulation. Second Order scheme was used for solving the pressure scheme and Second Order Upwind was used for both Momentum and Energy. Also, Least Square Cell-Based gradient was considered to solve the computational model. Numerical

solution controlled with the default Under-Relaxation Factors. Most of the models were got stability in terms of pressure which is under relaxed by a factor of 0.3. Standard initialization took place from the initial values of certain boundary conditions. The absolute convergence criterion was taken  $1 \times 10^{-6}$  for all of the residuals. It took around 2500-9000 iterations for falling all the residuals below the convergence tolerance  $1 \times 10^{-6}$ .

This study investigates only the heating effect of the heat exchangers. So, the wall temperature is higher than the flowing fluid inside the pipe. The boundary conditions for the geometrical effect analysis on the eighteen geometries are described as follows. Uniform constant velocity boundary condition is fixed at the inlet and applied normal to the boundary. Inlet velocity magnitude is  $U_{in} = 1.5 \text{ ms}^{-1}$  for all the cases. Moreover, no-slip condition is considered. For the air, the inlet temperature is taken  $T_{in} = 293.15 \text{ K}$ . Also, outlet pressure is taken as zero-gauge pressure,  $P_{out} = 0 \text{ Pa}$ . Constant wall temperature condition is applied for the study. For maintaining a large temperature difference and ensuring better analysis and observation of the effect, a relatively higher temperature of the wall temperature is taken. The constant wall temperature is  $T_{wall} = 423.15 \text{ K}$ . It is a laminar flow study, so no turbulence model or boundary condition took place.

**Table 4.1:** Geometrical parameters and fluid properties used in this study.

Parameters	Value	Unit
$T_{in}$	293.15	K
$T_{wall}$	423.15	K
d	0.0113	m
$h_c$	0.02	m

$R_c$	0.04	m
$L$	1.26	m
$C_{\rho,1}$	$5.28 \times 10^{-6}$	$\text{Kg m}^{-3} \text{K}^{-2}$
$C_{\rho,2}$	$-6.66 \times 10^{-3}$	$\text{Kg m}^{-3} \text{K}^{-1}$
$C_{\rho,3}$	2.70	$\text{Kg m}^{-3}$
$C_{\mu,1}$	$-2.47 \times 10^{-11}$	$\text{Kg m}^{-1} \text{s}^{-1} \text{K}^{-2}$
$C_{\mu,2}$	$6.15 \times 10^{-8}$	$\text{Kg m}^{-1} \text{s}^{-1} \text{K}^{-1}$
$C_{\mu,3}$	$2.29 \times 10^{-6}$	$\text{Kg m}^{-1} \text{s}^{-1}$
$C_{k,1}$	$-2.41 \times 10^{-8}$	$\text{W m}^{-1} \text{K}^{-3}$
$C_{k,2}$	$8.64 \times 10^{-5}$	$\text{W m}^{-1} \text{K}^{-2}$
$C_{k,3}$	$2.39 \times 10^{-3}$	$\text{W m}^{-1} \text{K}^{-1}$
$C_{cp,1}$	$3.54 \times 10^{-4}$	$\text{J kg}^{-1} \text{K}^{-3}$
$C_{cp,2}$	$-1.64 \times 10^{-1}$	$\text{J kg}^{-1} \text{K}^{-2}$
$C_{cp,3}$	$10.22 \times 10^2$	$\text{J kg}^{-1} \text{K}^{-1}$
$V_{in}$	1.5	$\text{ms}^{-1}$
$P_{out}$ (gauge)	0	Pa

---

In the study of the effect of nanofluid, all the boundary conditions are as same as above, except there is a wall coupled boundary condition between the two adjacent walls of the inner nanofluid pipe and the outer ribbed pipe. Water is used as base fluid in the outer pipe region instead of air. It is noted that there is no mixing of water and nanofluid, as there is a thin wall placed between these two. To ensure the flow as laminar the Reynolds numbers were taken less than 2000 for this study. The inlet velocity of water passing through the outer ribbed pipe and the nanofluid

passing through the inner ribbed pipe with different constant velocities placed in **Table 4.2**. The inlet temperature is also as same as before, 293.15 K. Zero-gauge pressure was taken for both of the pipes. Outer pipe wall temperature is 423.15K.

**Table 4.2:** Different inlet velocity of water at the outer pipe for nanofluid study

Velocity ( $\text{ms}^{-1}$ )	Reynolds Number (Re)	Dean Number (De)
0.05	634	237
0.1	1270	476
0.15	1904	714

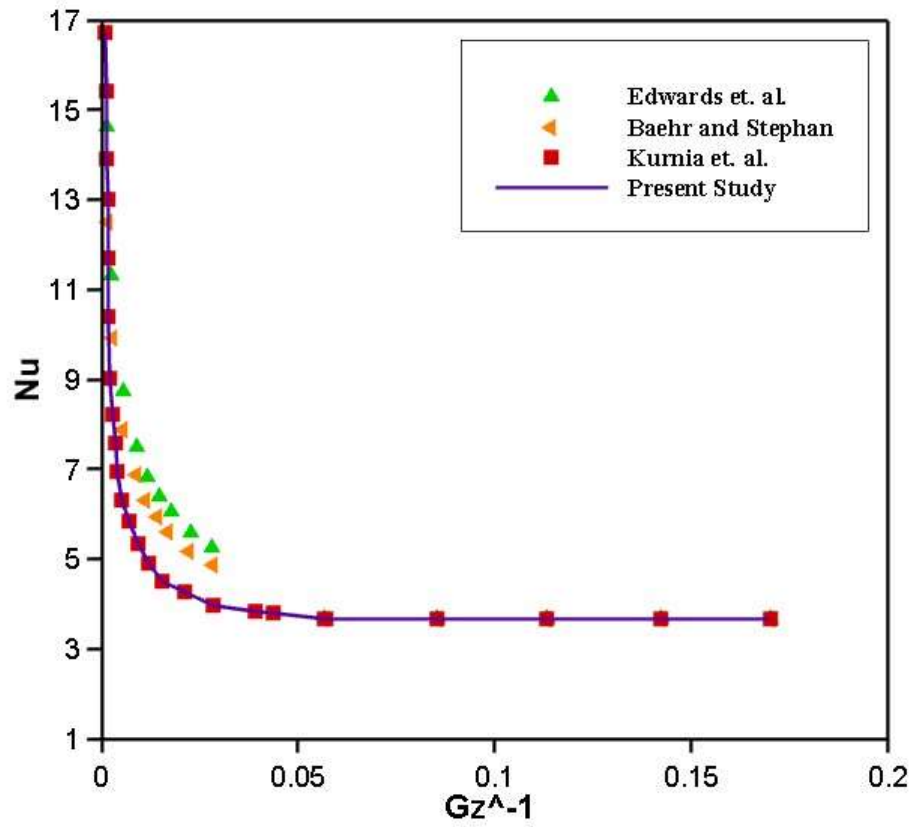
## ***CHAPTER 5:***

### ***RESULTS AND DISCUSSIONS***

Geometrical effect with three different ribbed profiles and three different coil revolutions are shown in this chapter. Velocity, temperature distribution and local Nusselt number comparison have been done to evaluate the geometrical effect properly. Finally, comparison among four different nanofluids applied in the best type of heat exchanger inserting a circular pipe is shown and discussed.

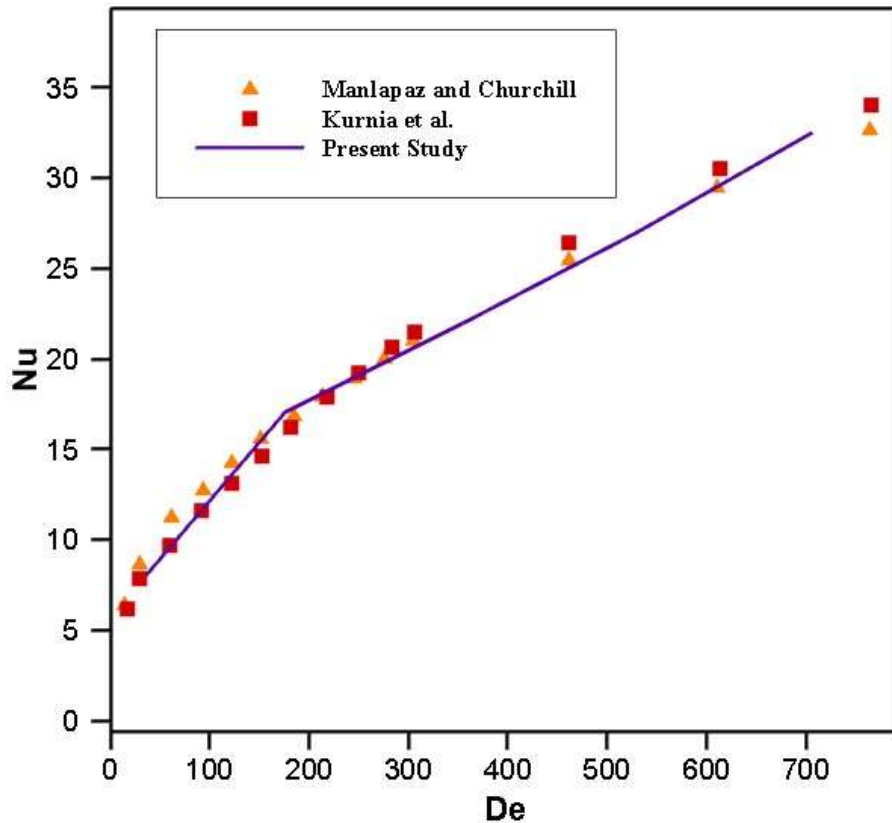
#### **5.1. Model validation**

The numerical studies were validated against some experimental correlations and numerical simulations. Analysis of straight pipe was validated against the numerical study done by Kurnia et al. [1] and two experimental correlations done by Edwards et al. [21] and Baehr and Stephan [22] respectively shown in the **Figure 5.1(a)**. This is about the local Nusselt number comparison throughout the whole pipe. On the other hand, for the helical geometries, Nusselt number with a variation of Dean number has been shown and validated against a numerical study done by Kurnia et al. [1] and an experimental correlation by Manlapaz and Churchill [23] which is represented in **Figure 5.1(b)**. It is observed that less than 4% relative error for both the geometries while validated from the experimental correlation and 1% relative error for the numerical study. So, this small amount of relative error was taken in consideration to proceed further in this present study.



(a)





(b)

**Figure 5.1** Validation graph of (a) Nu vs  $Gz^{-1}$  plot for straight pipes (b) Nu vs De plot for helical pipes

## 5.2. Effect of geometry in terms of helical or straight

There are significant variations in the velocity and temperature distributions across the heat exchangers. The numerical simulation results show the effect of the geometry of the helical and straight pipes. For observation, contours were plotted at the same distance of 250mm from the inlet in all the geometries which are shown in [Figure 5.2](#) Velocity distribution of helical heat

exchangers of all 9 cases has been shown and it is observed that the higher the ribbed geometry higher the velocity due to curvature, also the higher the revolution higher the velocity across the pipe.

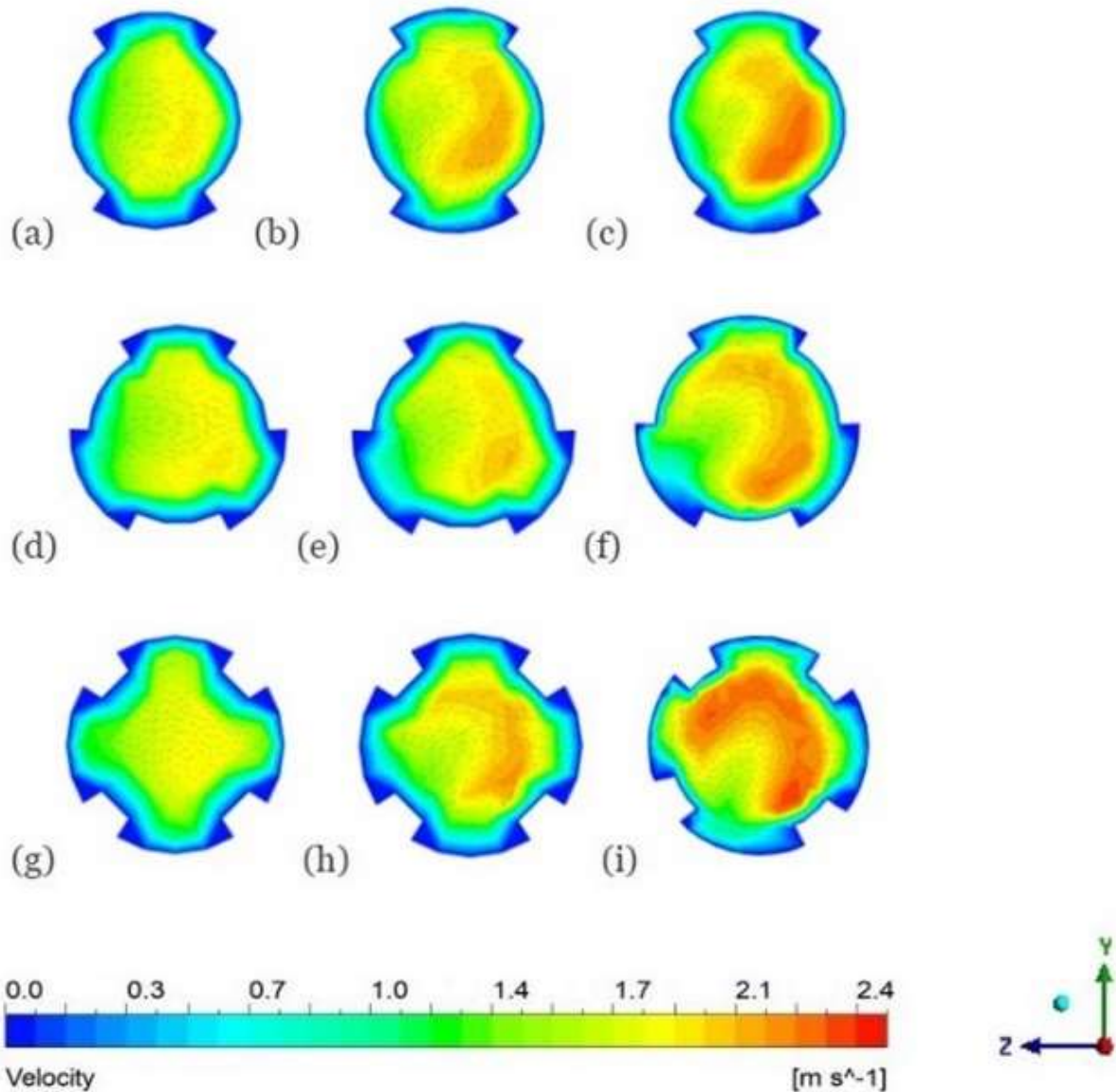


**Figure 5.2** Axial velocity profile contour in helical heat exchanger of (a) Case 1 (b) Case 2 (c) Case 3 (d) Case 4 (e) Case 5 (f) Case 6 (g) Case 7 (h) Case 8 (i) Case 9 at  $L= 250\text{mm}$

Similarly, **Figure 5.3** shows the axial velocity contour plot for all the 9 cases of straight-type heat exchangers. It is observed that the axial velocity is higher at the middle portion of the straight pipes. Velocity is higher in a straight type heat exchanger than a helical heat exchanger due to less amount of friction loss.

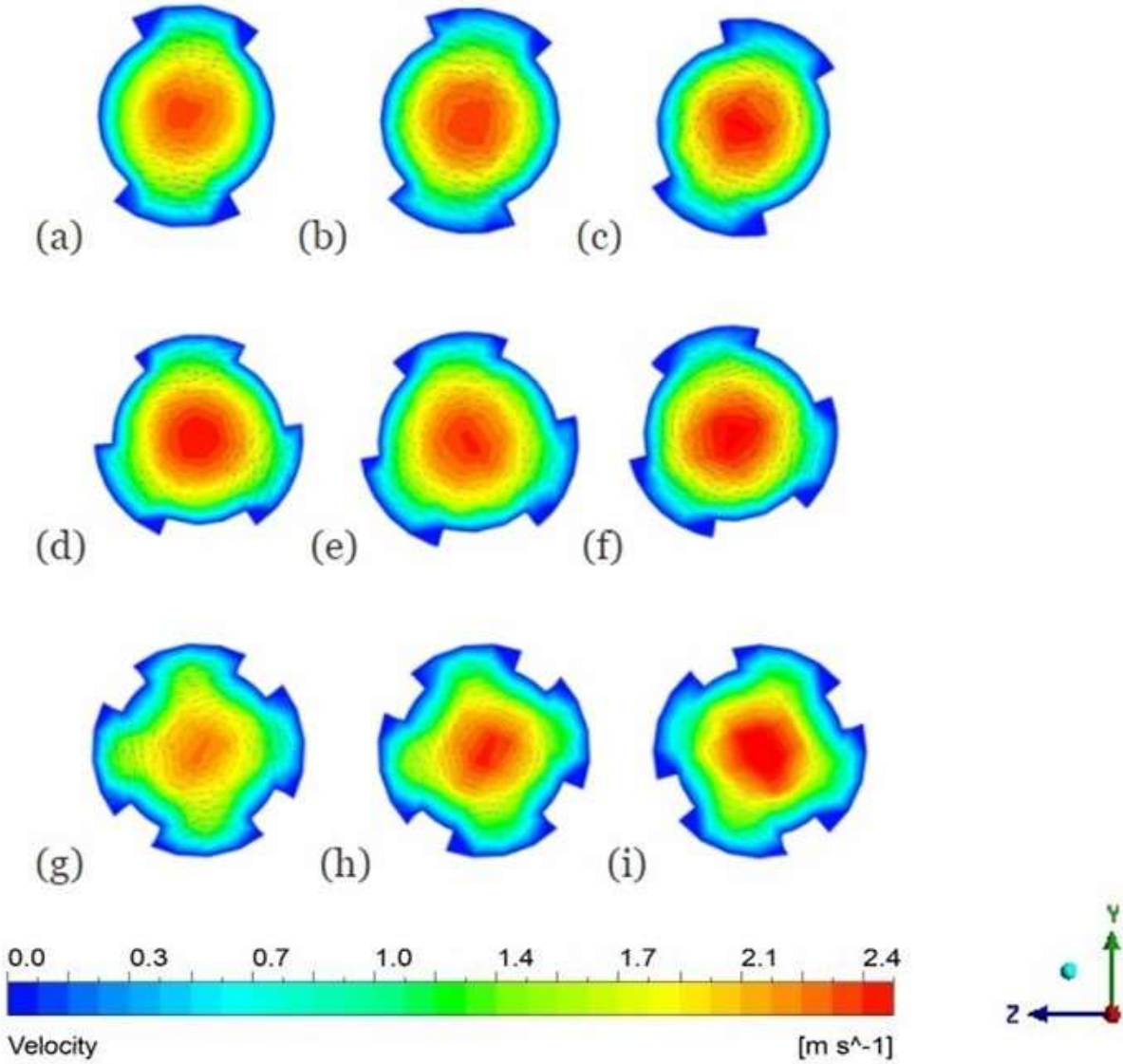


**Figure 5.3** Axial velocity profile contour in straight heat exchanger of (a) Case 1 (b) Case 2 (c) Case 3 (d) Case 4 (e) Case 5 (f) Case 6 (g) Case 7 (h) Case 8 (i) Case 9 at L= 250mm

In all the geometries, everywhere there will not be the same temperature. After passing through some distance the temperature of the fluid will change accordingly. As it is a heating case so it is expected that the temperature is higher on the outer side of the wall. **Figure 5.4** shows the temperature distribution at the distance of 250mm from the inlet. It is found that there is a significant effect of ribbed revolutions. Higher the ribbed profile revolutions higher the temperature in a particular distance contour plot.

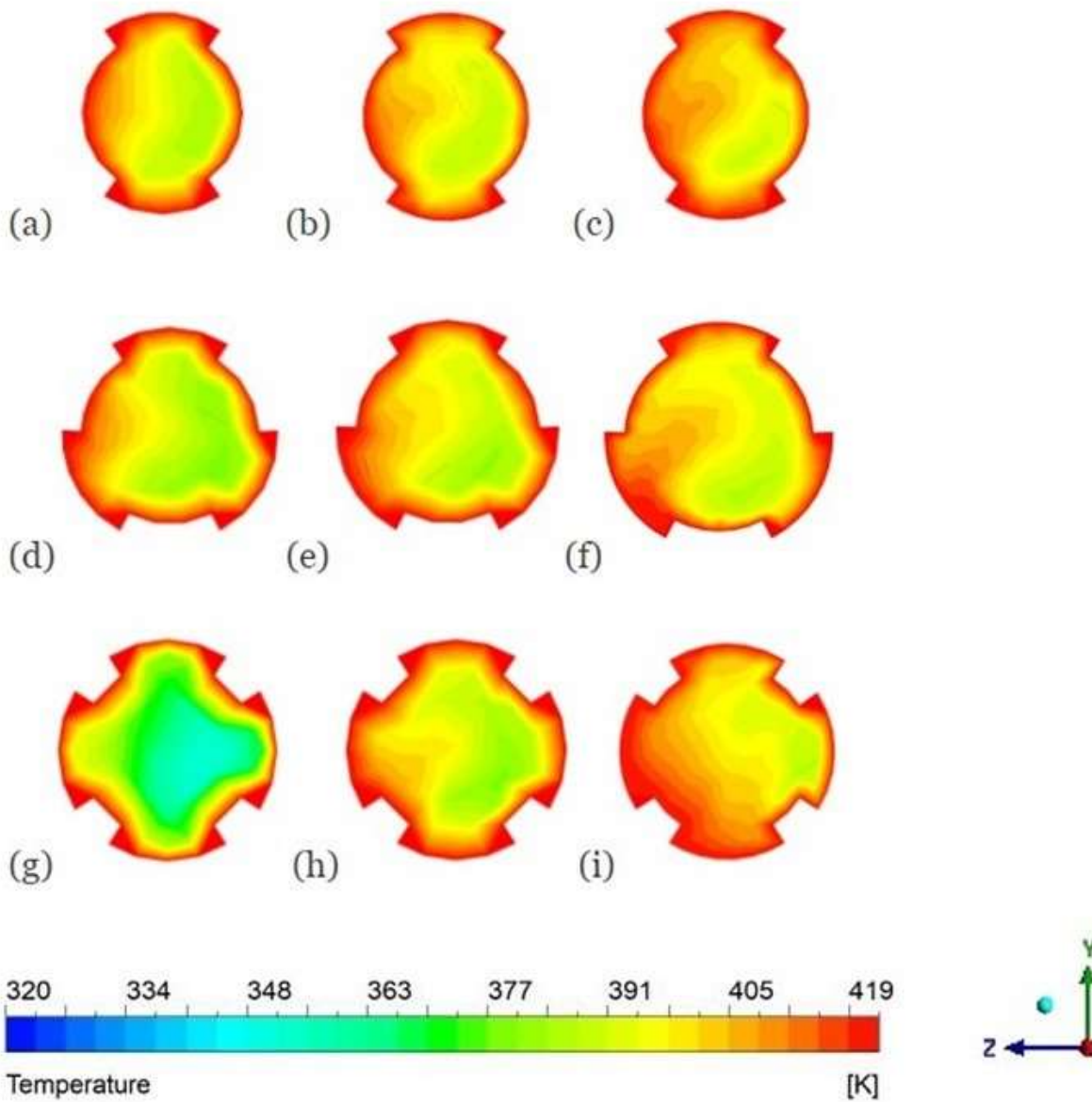


**Figure 5.4** Temperature distribution contour in helical heat exchanger of (a) Case 1 (b) Case 2 (c) Case 3 (d) Case 4 (e) Case 5 (f) Case 6 (g) Case 7 (h) Case 8 (i) Case 9 at  $L= 250\text{mm}$

For the straight heat exchangers, the temperature distributions are not that much higher than the helical heat exchangers. But in [Figure 5.5](#) it is observed that the higher the coil revolution of the pipe higher the temperature at a certain distance of the pipe.

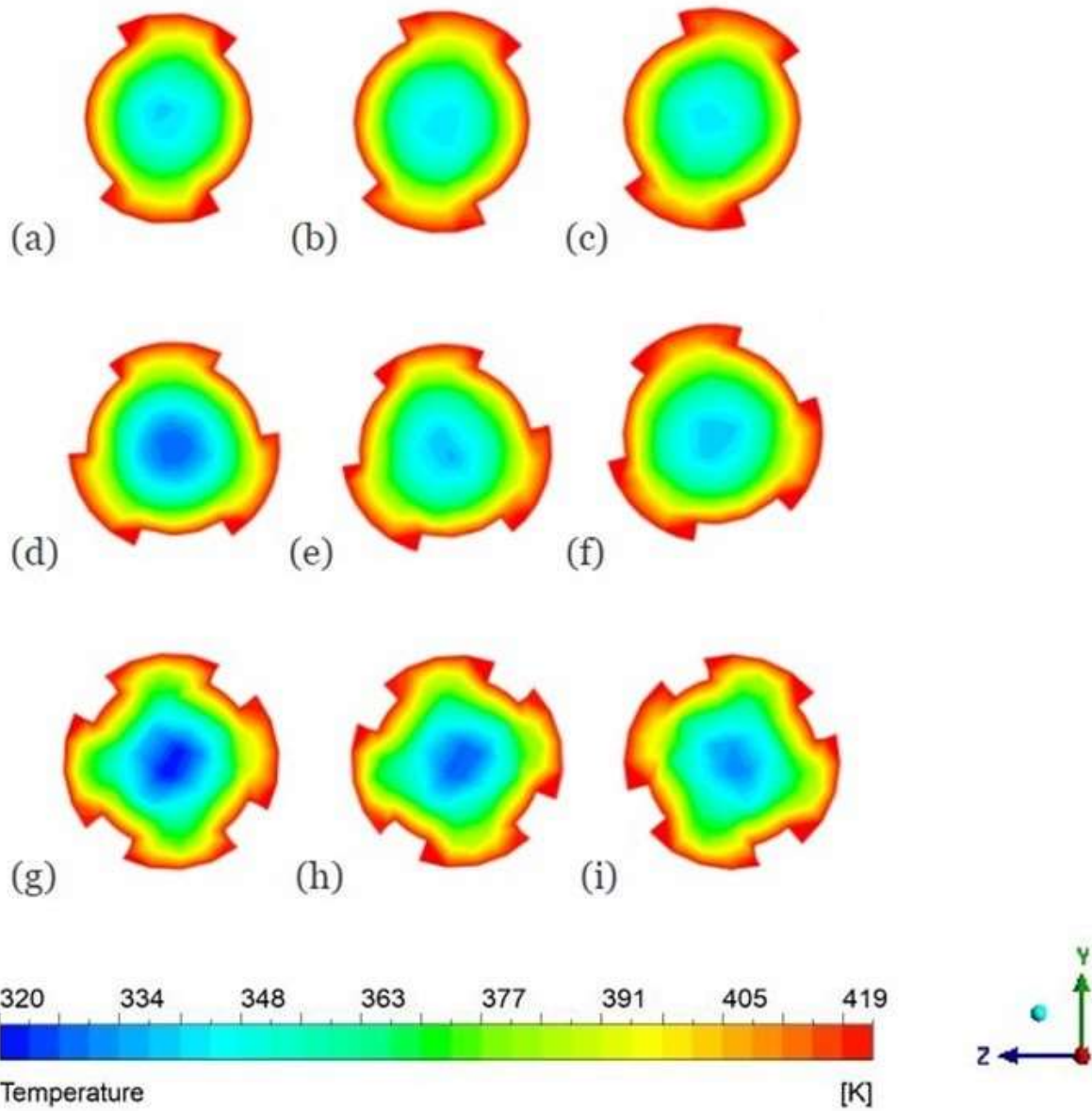
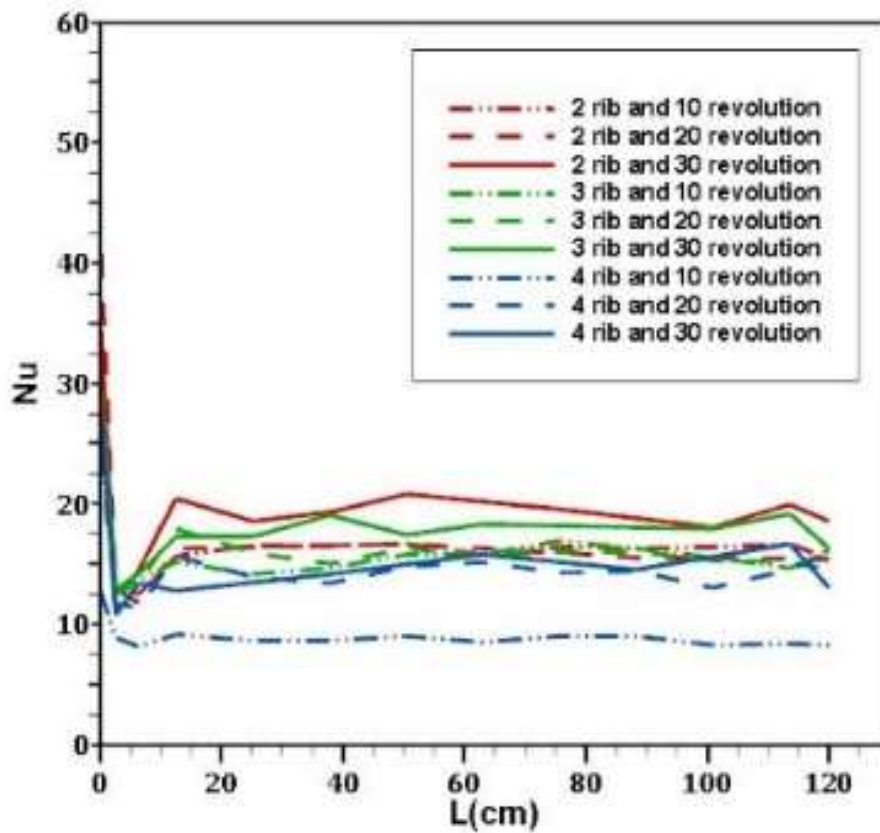


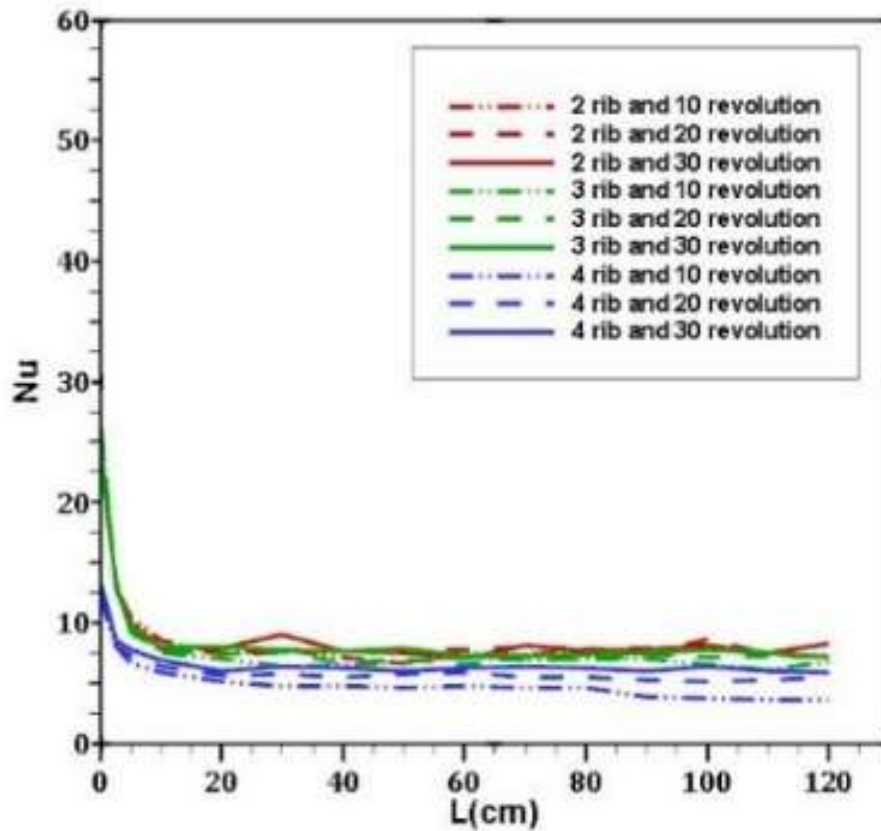
**Figure 5.5** Temperature distribution contour in straight heat exchanger of (a) Case 1 (b) Case 2 (c) Case 3 (d) Case 4 (e) Case 5 (f) Case 6 (g) Case 7 (h) Case 8 (i) Case 9 at  $L= 250\text{mm}$

Helical heat exchanger is more effective than a straight type of heat exchanger. [Figure 5.6](#) shows

the heat transfer comparison between helical and straight types of heat exchangers. It is clearly seen that the helical heat exchanger has a higher local Nusselt number than the straight type of heat exchanger with the same ribbed head profile and coil revolutions. It is noted that with the same ribbed head number and coil revolutions, 2 ribbed 30 revolutions helical heat exchanger gave 2 times higher Nusselt number than the straight type heat exchanger.



(a)



(b)

**Figure 5.6** Nusselt number vs local distance plot of (a) helical pipes with (b) straight pipes

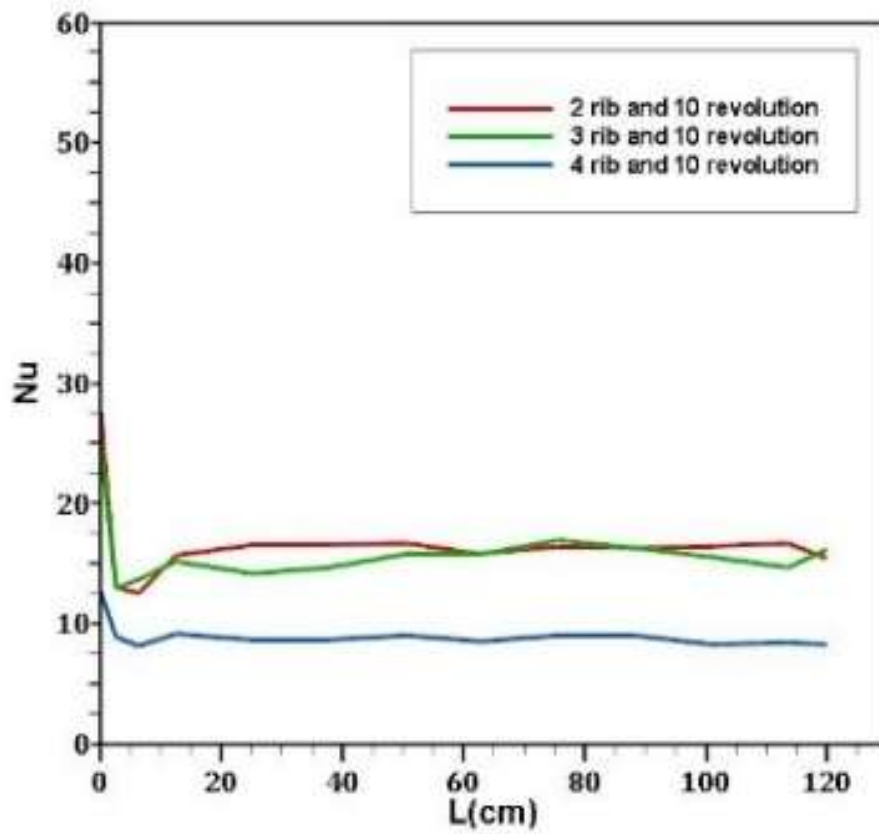
From the graphs, it can be said that the two head ribbed with 30 coil revolutions helical heat exchanger ensures the highest amount of heat transfer rate. And four head ribbed with 10 coil revolution straight tube heat exchanger has got the lowest value of heat transfer rate.

### 5.3. Effect of ribbed profile

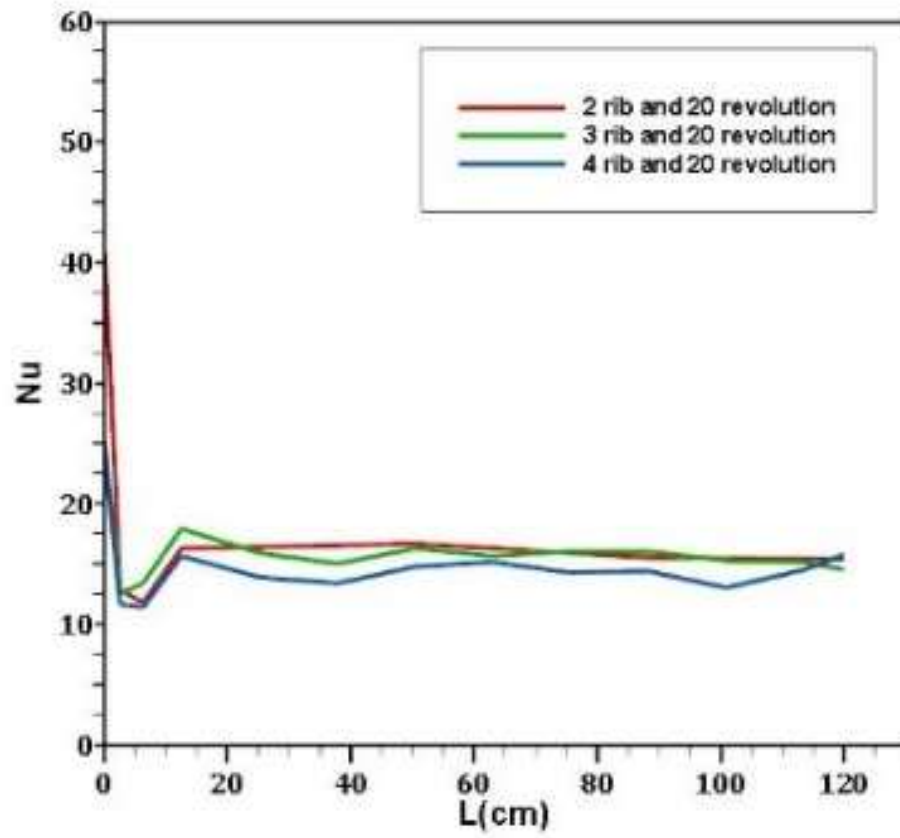
From eqn 17, it can be said that the higher the surface area of the heat exchanger higher the heat



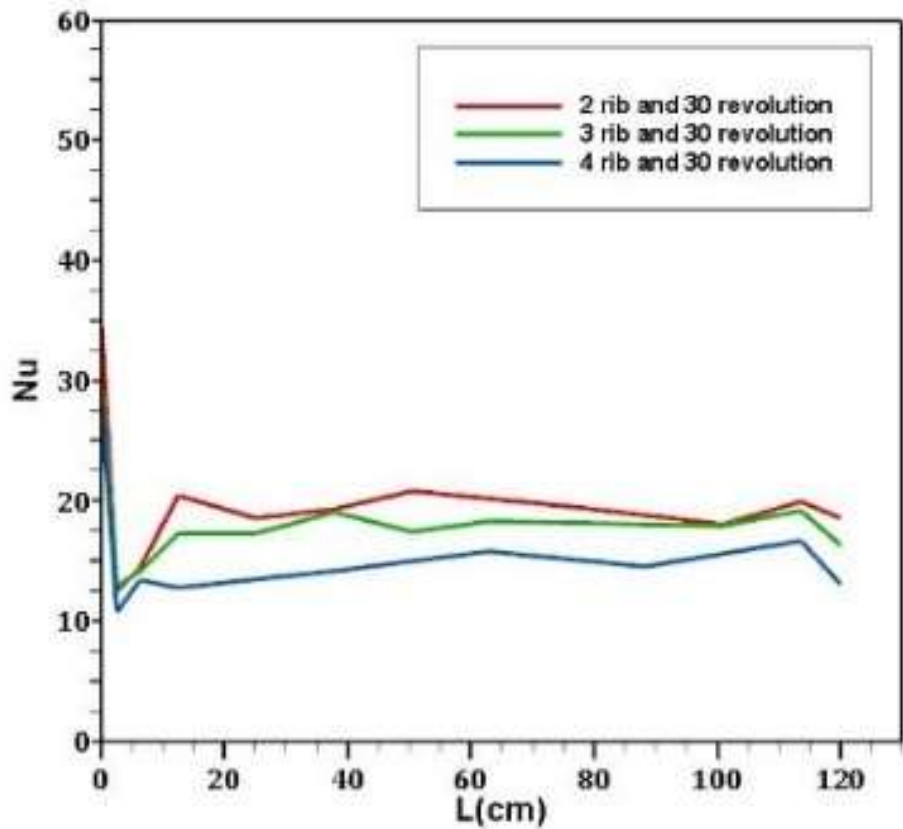
transfer rate. To get a larger wetted perimeter of the cross-section, ribbed geometry profiles can be introduced. The present study deals with the geometrical effect of the heat exchanger and ribbed geometry profiles play a good role in enhancing the heat transfer rate for both helical and straight pipe. Xu et. al [16] investigated that ribbed profile geometry transfers heat 1.05-1.35 times higher than the plain tube. In the helical heat exchanger, the ribbed geometry ensures a significant amount of mixing due to present of curvatures. Curvature ensures better mixing and mixing enhances the heat dissipation resulting in increasing the heat transfer rate. **Figure 5.7** shows the ribbed geometry effect in helical heat exchangers and **Figure 5.8** shows the ribbed geometry effect in straight heat exchangers. It is observed that taking the same revolution turn of the ribbed geometry, the two head ribbed heat exchanger has the highest heat transfer rate. Four head ribbed geometry has given the lowest heat transfer rate. **Figure 5.7(a)** represents the constant 10 revolutions



(a)



(b)

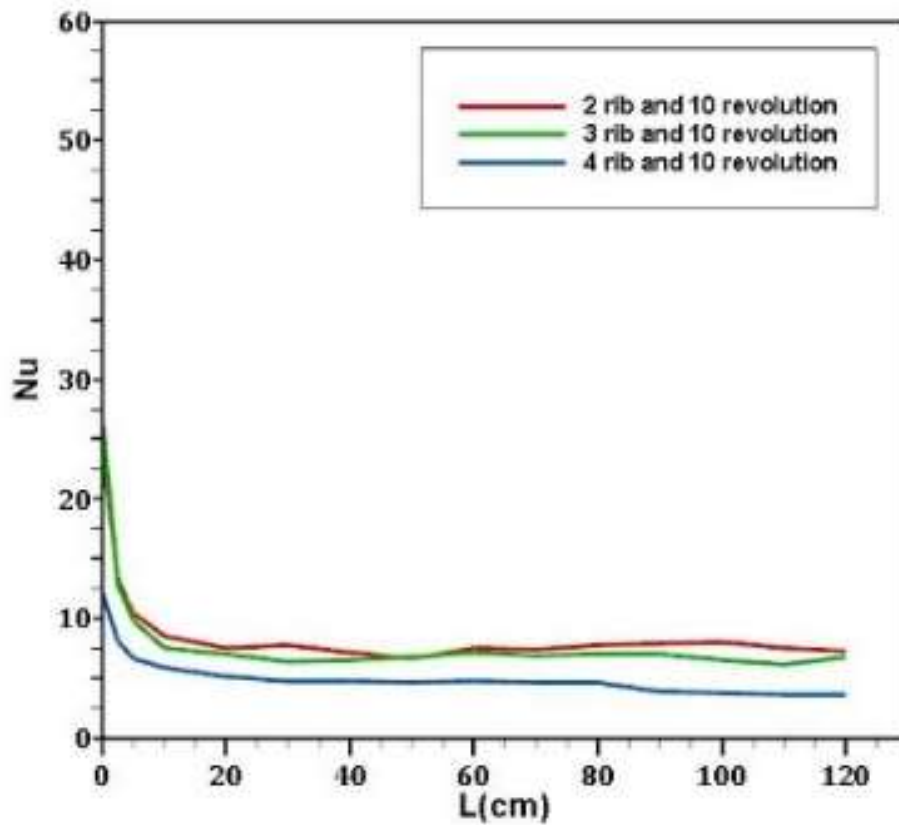


(c)

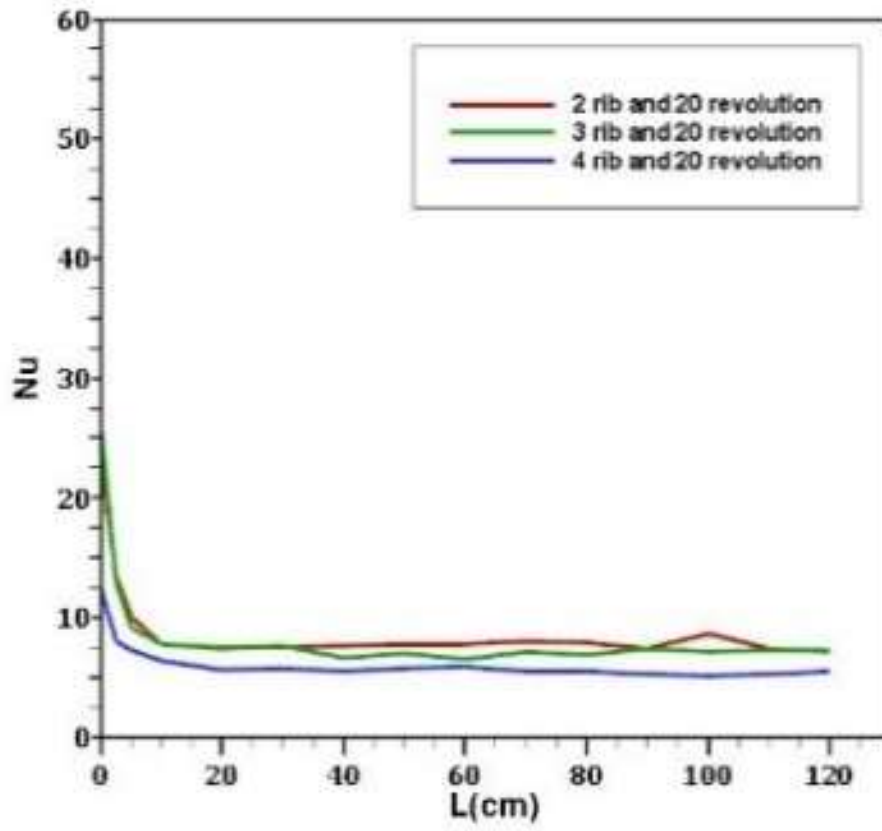
**Figure 5.7** Nusselt number vs local distance plot of helical heat exchanger with (a) 10 revolution (b) 20 revolution (c) 30 revolution

For a straight heat exchanger, it can be noticed the effect of ribbed geometry as well. It is no wonder that for straight heat exchanger the same result. [Figure 5.8\(a\)](#) represents the constant 10 revolutions with 2 head ribbed, 3 head ribbed, and 4 head ribbed geometry of straight heat exchangers. It can be seen that the 2 head ribbed 10 revolution ensures the highest Nusselt

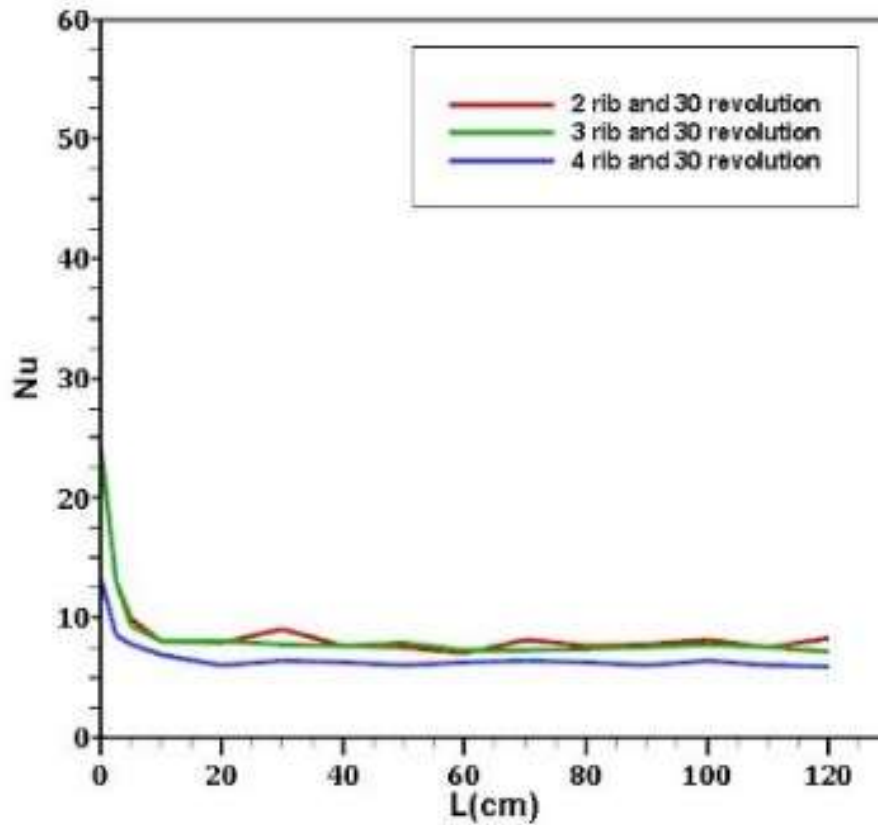
number throughout the pipe. Similarly, **Figure 5.8(b)** represents the constant 20 revolutions with 2 head ribbed, 3 head ribbed, and 4 head ribbed geometry of straight heat exchangers. It is observed that 2 head ribbed 20 revolution has the highest heat transfer rate. **Figure 5.8(c)** represents the constant 30 revolutions with 2 head ribbed, 3 head ribbed, and 4 head ribbed geometry of straight heat exchangers. The result shows that 2 head ribbed 30 revolution has the highest heat transfer rate. So it can be concluded that the lesser the rib head number higher the heat transfer rate for both helical and straight heat exchangers.



(a)



(b)



(c)

**Figure 5.8** Nusselt number vs local distance plot of straight pipe with (a) 10 revolution (b) 20 revolution (c) 30 revolution

#### 5.4. Effect of coil revolution

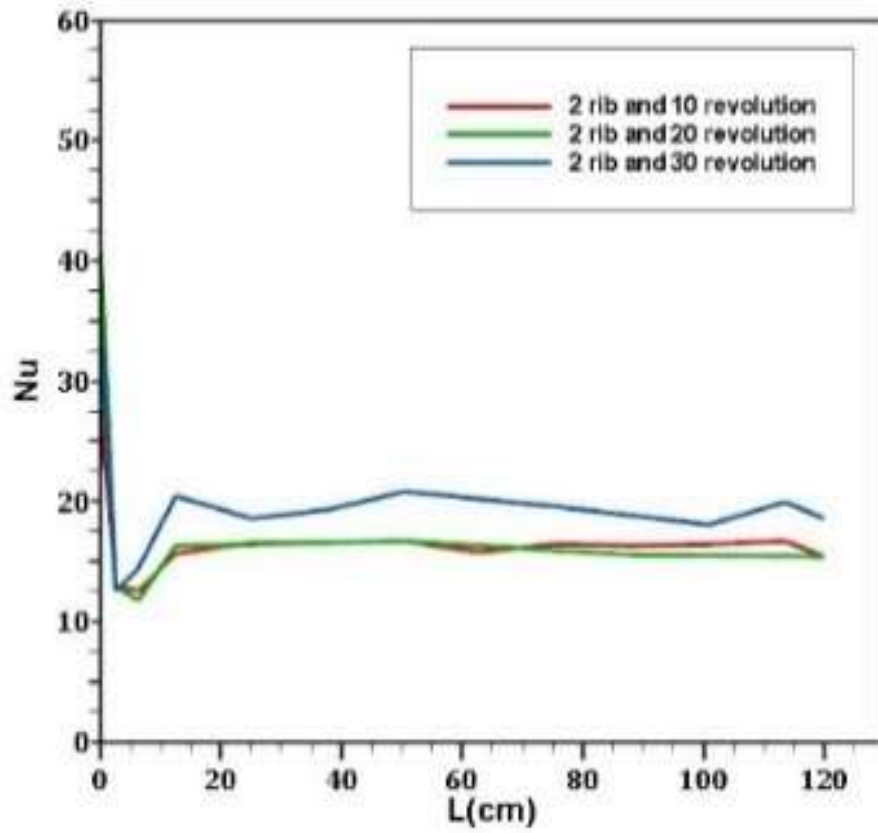
The unique design introduces helical ribbed structure in the helical and straight heat exchangers. Previously shown that the ribbed profile enhances heat transfer rate and lesser the rib profile head number higher the heat transfer rate. So, the goal is to observe the effect of coil revolution

of the ribbed geometry.

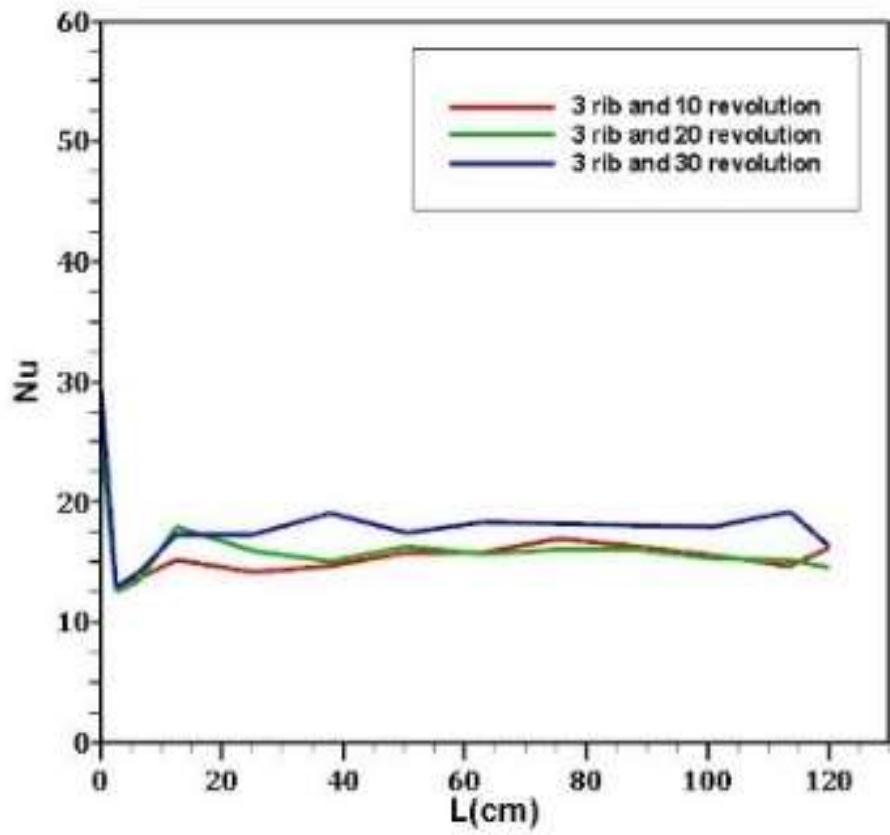
Higher the coil revolution higher the curvature ensured in the heat exchanger. **Figure 5.9** and **Figure 5.10** shows that the effect of coil revolution in helical and straight heat exchanger respectively. It is observed that taking same ribbed profile, higher the coil revolution, higher the heat transfer rate. So, the 30 revolution has given the highest heat transfer rate.

**Figure 5.9 (a)** represents the constant 2 head ribbed with 10 revolutions, 20 revolutions, and 30 revolutions geometry of helical heat exchangers. It is seen that the 2 head ribbed 30 revolution ensures the highest Nusselt number throughout the pipe. Similarly, **Figure 5.9 (b)** represents the constant 3 head ribbed with 10 revolutions, 20 revolutions, and 30 revolutions geometry of helical heat exchangers. It is observed that 3 head ribbed 30 revolution has the highest heat transfer rate. **Figure 5.9 (c)** shows the constant 4 head ribbed with 10 revolutions, 20 revolutions, and 30 revolutions geometry of helical heat exchangers. It is observed that 4 head ribbed 30 revolution has the highest heat transfer rate.

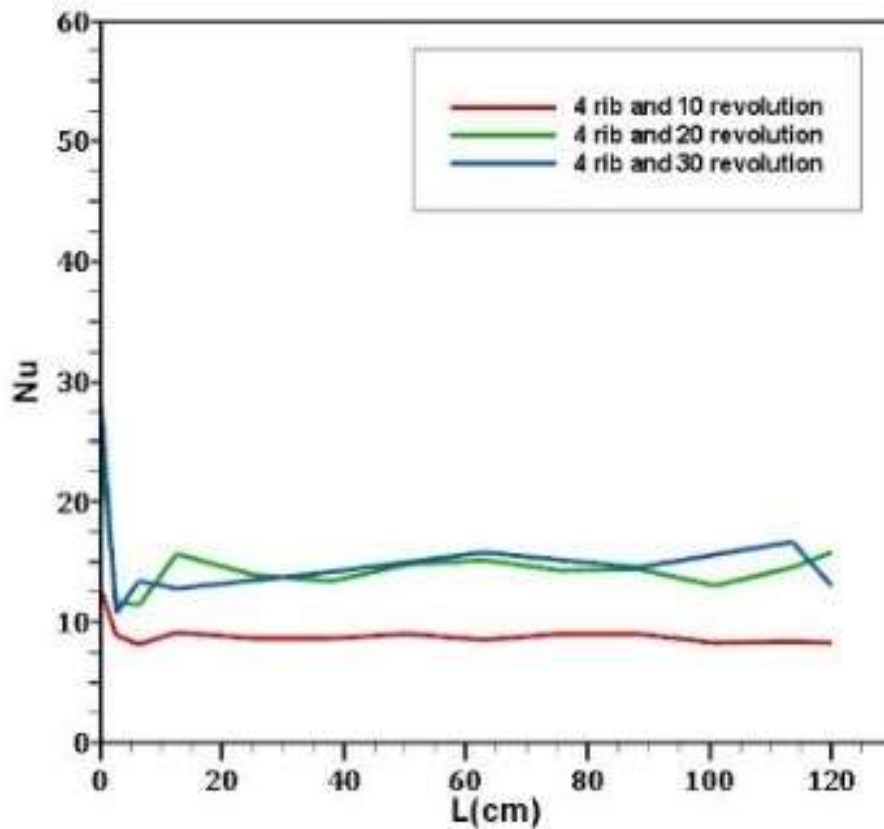




(a)



(b)

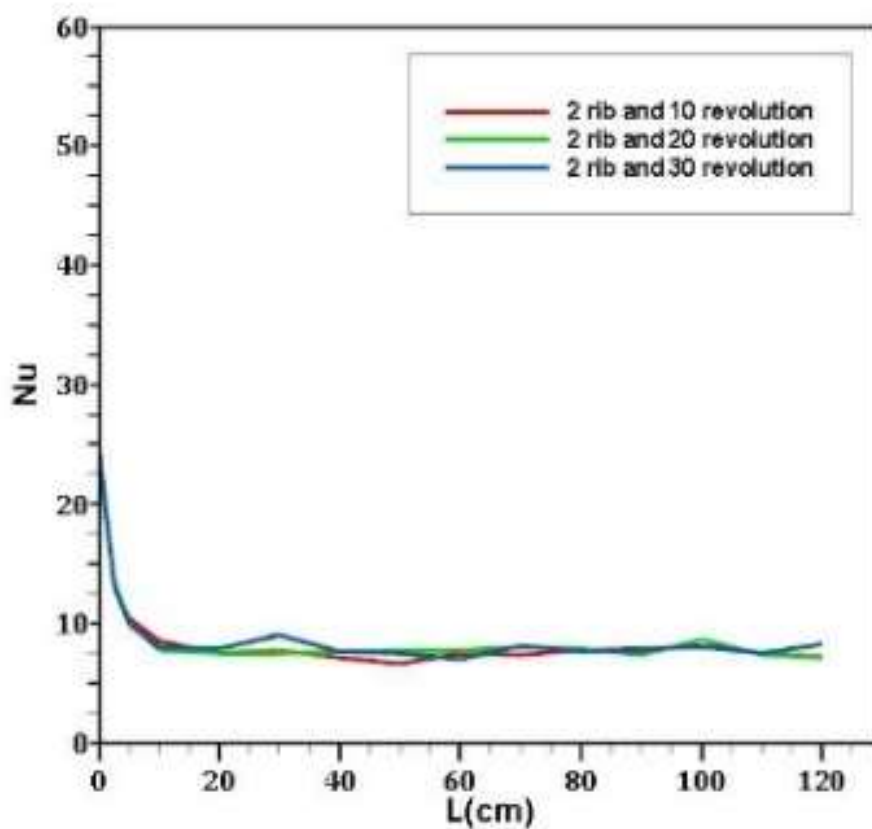


(c)

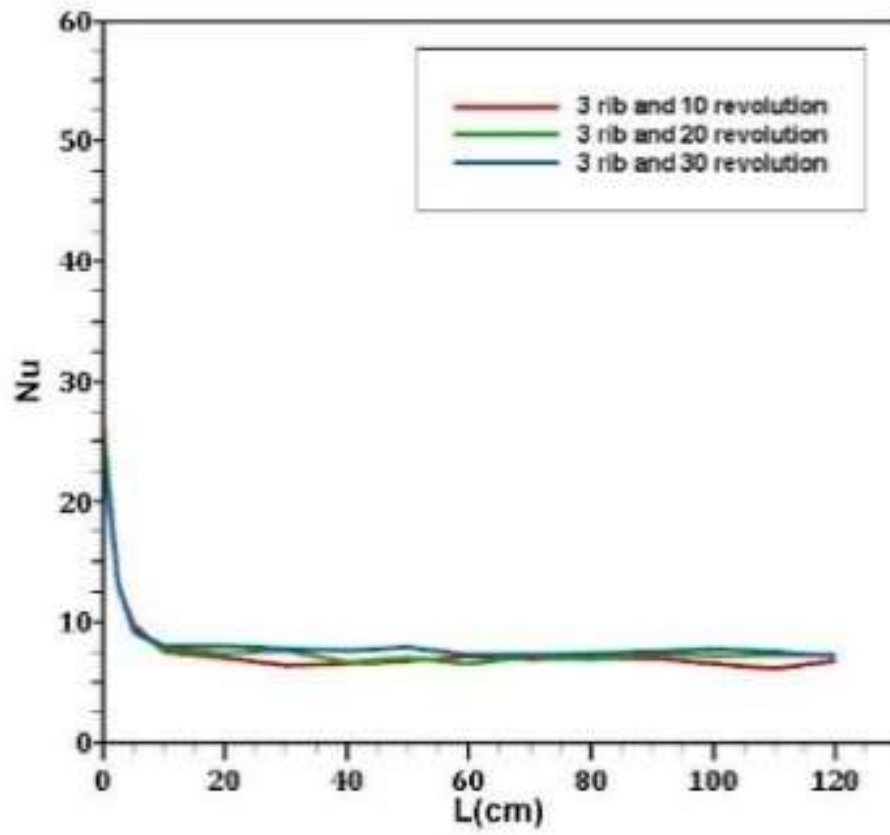
**Figure 5.9** Nusselt number vs local distance plot of helical pipe with (a) two-head ribbed (b) three-head ribbed (c) four-head ribbed with different revolutions

**Figure 5.10 (a)** represents the constant 2 head ribbed with 10 revolutions, 20 revolutions, and 30 revolutions geometry of straight heat exchangers. It is seen that the 2 head ribbed 30 revolution ensures the highest Nusselt number throughout the pipe. Similarly, **Figure 5.10 (b)** shows the constant 3 head ribbed with 10 revolutions, 20 revolutions, and 30 revolutions geometry of

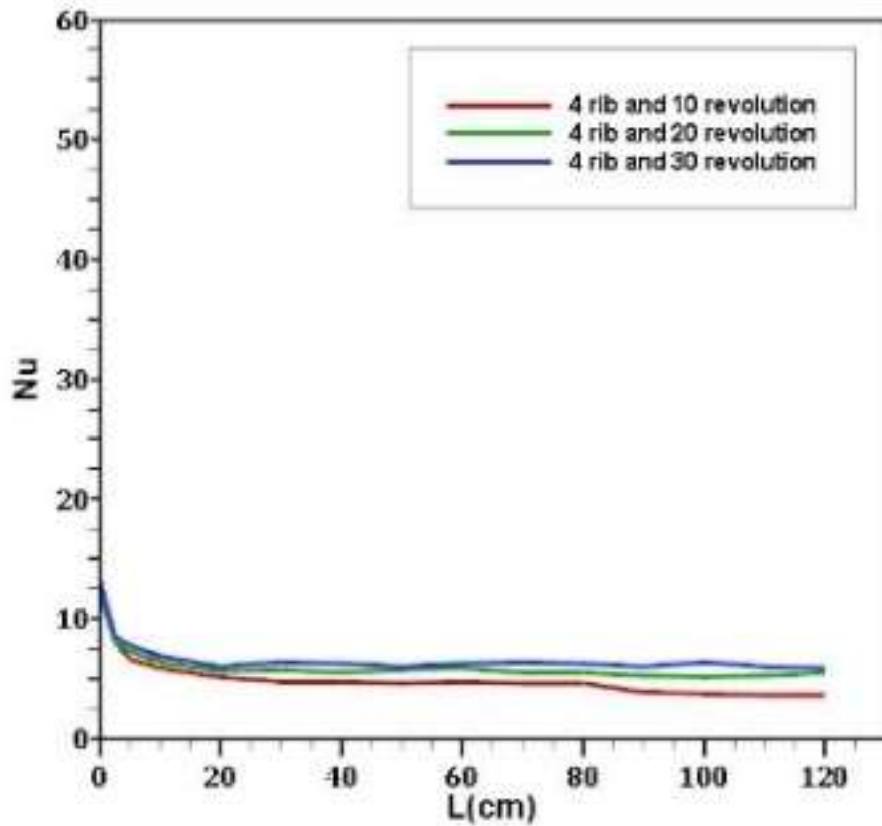
straight heat exchangers. It is observed that 3 head ribbed 30 revolution has the highest heat transfer rate. **Figure 5.10 (c)** represents the constant 4 head ribbed with 10 revolutions, 20 revolutions, and 30 revolutions geometry of straight heat exchangers. It is observed that 4 head ribbed 30 revolution has the highest heat transfer rate. So it is concluded that the higher the coil revolutions higher the heat transfer rate for both the helical and straight heat exchangers.



(a)



(b)



(c)

**Figure 5.10** Nusselt number vs local distance plot of straight pipe with (a) two-head ribbed (b) three-head ribbed (c) four-head ribbed with different revolutions.

### 5.5. Comparison of Nanofluid

So far, all the geometrical effects have been shown and from the obtained result it is clear that 2 head ribbed and 30 revolution helical heat exchanger has the highest local Nusselt number which

means it is the best heat exchanger among the 18 geometries. A numerical study has been done on this heat exchanger inserting a circular pipe inside it using four different nanofluids. The water-based nanofluid  $\text{Al}_2\text{O}_3$ ,  $\text{CuO}$ ,  $\text{SiO}_2$ ,  $\text{ZnO}$  were used for the observation of the nanofluid effect. It is one kind of tube in tube heat exchanger where the nanofluids pass through the inside circular pipe and water pass through the outer pipe of the heat exchanger.

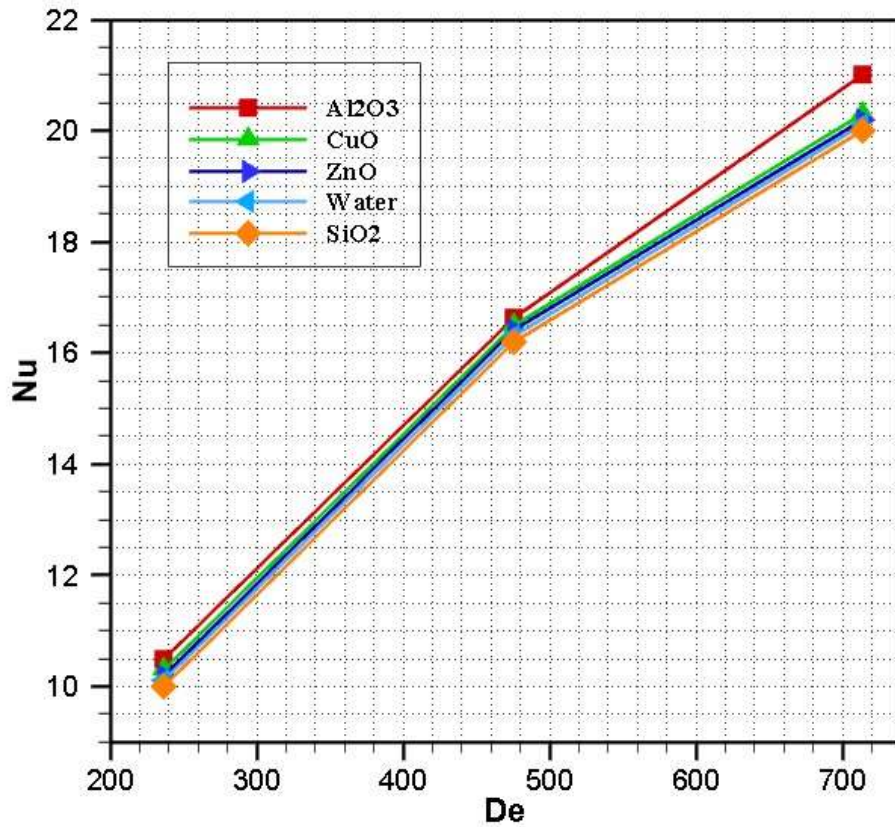


**Figure 5.11** Nusselt number vs Dean number plot for water based nanofluids

**Figure 5.11** shows the nanofluid effect on the heat exchanger in terms of total Nusselt number and Dean number. First of all, it is observed that increasing the Dean number the total Nusselt number also increases for all the nanofluids and water as well. Also, it is found that among four different nanofluids  $\text{Al}_2\text{O}_3$  has the highest heat transfer rate and  $\text{CuO}$  has the lowest Nusselt

number varying the Dean number.

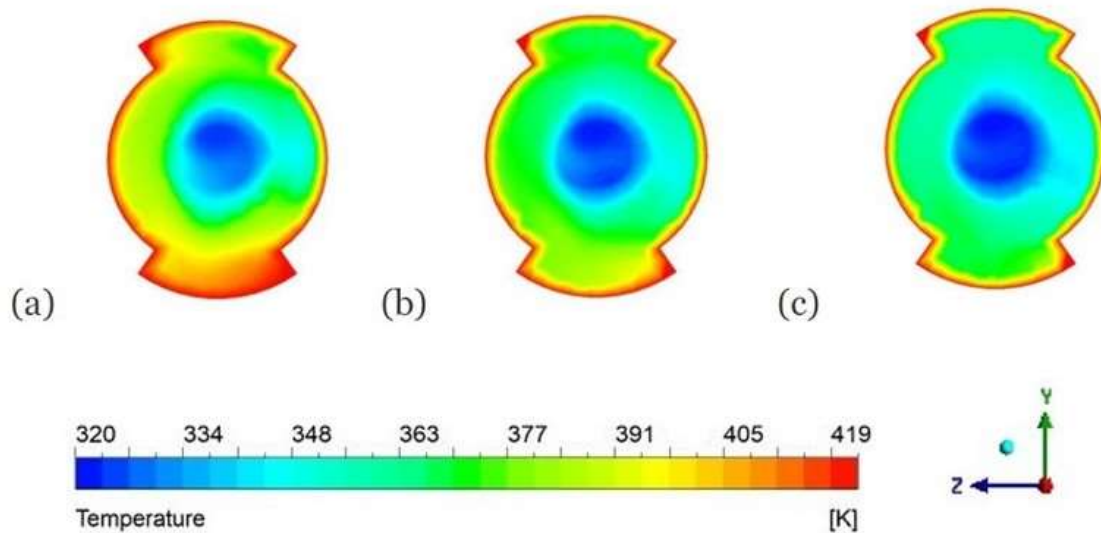


**Figure 5.12** Temperature distribution of tube in tube heat exchanger of (a)  $De= 237$  (b)  $De= 476$  (c)  $De= 714$  at  $L=250\text{mm}$ . Dean number has the significant effect of Nusselt number, **Figure 5.12** represents the temperature distribution of the  $\text{Al}_2\text{O}_3$  water based nanofluid with three different Dean number of 237, 476 and 714 at the distance of 250mm from inlet.



## ***CHAPTER 6:***

### **CONCLUSION:**

This study investigates the geometrical effect on a helical heat exchanger and straight heat exchangers. The numerical simulation was validated against several experimental correlations and numerical simulations. Further study was evaluated changing the geometry of the heat exchanger shape. Two different variable rib head and coil revolution were taken to observe the geometrical effect. 2 head ribbed, 3 head ribbed, and 4 head ribbed were taken and 10 revolutions, 20 revolutions, 30 revolutions were taken. It is found that the lesser the ribbed geometry higher the heat transfer rate resulting in 2 head ribbed geometries was most effective than the 3 head ribbed and 4 head ribbed. Also, the higher the coil revolution of the rib profile higher the heat transfer rate resulting in 30 revolutions has given the higher local Nusselt number than the 20 revolutions and 10 revolutions. So, the most effective geometry among the total 18 geometry is 2 head ribbed 30 revolutions helical heat exchanger. It is found that a helical heat exchanger is more effective than a straight heat exchanger, for some cases it is 2 times higher even. Implying nanofluid of  $\text{Al}_2\text{O}_3$ ,  $\text{CuO}$ ,  $\text{SiO}_2$ ,  $\text{ZnO}$  inside the best heat exchanger it is observed that  $\text{Al}_2\text{O}_3$  water-based nanofluid gives the highest Nusselt number across the pipe. Further study can be done using turbulence in the heat exchangers.

## Nomenclature:

$A_c$	=	Cross	sectional	area
$A_s$	=		Surface	area
$C_p$	=		Specific	heat
$\mu$	=		Dynamic	viscosity
$\rho$	=			Density
$D_h$	=		Hydraulic	diameter
$g$	=		Gravitational	acceleration
Re	=	Reynolds number ( $=\frac{\rho V D_h}{\mu}$ )		
De	=	Dean	Number	( $= Re \sqrt{\frac{D_h}{2R_c}}$ )
Gz	=	Graetz	number	( $=\frac{D_h}{L} Re Pr$ )
Pr	=	Prandtl	number	( $=\frac{c_p k}{\mu}$ )
Nu	=	Nusselt	number	( $=\frac{h D_h}{k}$ )
$h$	=	Heat	transfer	coefficient
$h_c$	=		Coil	pitch
$k$	=		Thermal	conductivity
$L$	=		Tube	length
$P$	=			Pressure
$Q_{total}$	=	Total	heat transfer	rate

$Q_{wall}$	=	Wall	heat	flux
$R_c$	=	Coil		radius
$T$	=			Temperature
$T_{in}$	=	Inlet		temperature
$T_{out}$	=	Outlet		temperature
$T_{mean}$	=	Mean		Temperature
$T_{wall}$	=	Wall		temperature
$V_{in}$	=	Inlet		velocity
$V$	=			Velocity
$\dot{m}$	=	Mass	flow	rate

LMTD= Log Mean Temperature Difference

## **REFERENCES:**

- [1] J. C. Kurnia, A. P. Sasmito, T. Shamim, and A. S. Mujumdar, “Numerical investigation of heat transfer and entropy generation of laminar flow in helical tubes with various cross sections,” *Appl. Therm. Eng.*, vol. 102, pp. 849–860, 2016, doi: 10.1016/j.applthermaleng.2016.04.037.
- [2] M. Farzaneh-Gord, H. Ameri, and A. Arabkoohsar, “Tube-in-tube helical heat exchangers performance optimization by entropy generation minimization approach,” *Appl. Therm. Eng.*, vol. 108, pp. 1279–1287, 2016, doi: 10.1016/j.applthermaleng.2016.08.028.
- [3] T. Srinivas and A. Venu Vinod, “Performance of an agitated helical coil heat exchanger using Al<sub>2</sub>O<sub>3</sub>/water nanofluid,” *Exp. Therm. Fluid Sci.*, vol. 51, pp. 77–83, 2013, doi: 10.1016/j.expthermflusci.2013.07.003.
- [4] K. Narrein and H. A. Mohammed, “Influence of nanofluids and rotation on helically coiled tube heat exchanger performance,” *Thermochim. Acta*, vol. 564, pp. 13–23, 2013, doi: 10.1016/j.tca.2013.04.004.
- [5] M. A. Khairul, R. Saidur, M. M. Rahman, M. A. Alim, A. Hossain, and Z. Abdin, “Heat transfer and thermodynamic analyses of a helically coiled heat exchanger using different types of nanofluids,” *Int. J. Heat Mass Transf.*, vol. 67, pp. 398–403, 2013, doi: 10.1016/j.ijheatmasstransfer.2013.08.030.
- [6] T. Srinivas and A. Venu Vinod, “Heat transfer intensification in a shell and helical coil

- heat exchanger using water-based nanofluids,” *Chem. Eng. Process. Process Intensif.*, vol. 102, pp. 1–8, 2016, doi: 10.1016/j.cep.2016.01.005.
- [7] N. Kannadasan, K. Ramanathan, and S. Suresh, “Comparison of heat transfer and pressure drop in horizontal and vertical helically coiled heat exchanger with CuO/water based nano fluids,” *Exp. Therm. Fluid Sci.*, vol. 42, pp. 64–70, 2012, doi: 10.1016/j.expthermflusci.2012.03.031.
- [8] J. Fernández-Seara, C. Piñeiro-Pontevedra, and J. A. Dopazo, “On the performance of a vertical helical coil heat exchanger. Numerical model and experimental validation,” *Appl. Therm. Eng.*, vol. 62, no. 2, pp. 680–689, 2014, doi: 10.1016/j.applthermaleng.2013.09.054.
- [9] C. Gnanavel, R. Saravanan, and M. Chandrasekaran, “Heat transfer augmentation by nano-fluids and Spiral Spring insert in Double Tube Heat Exchanger-A numerical exploration,” *Mater. Today Proc.*, vol. 21, no. xxxx, pp. 857–861, 2020, doi: 10.1016/j.matpr.2019.07.602.
- [10] G. Humnic and A. Humnic, “Heat transfer characteristics in double tube helical heat exchangers using nanofluids,” *Int. J. Heat Mass Transf.*, vol. 54, no. 19–20, pp. 4280–4287, 2011, doi: 10.1016/j.ijheatmasstransfer.2011.05.017.
- [11] V. Kumar, S. Saini, M. Sharma, and K. D. P. Nigam, “Pressure drop and heat transfer study in tube-in-tube helical heat exchanger,” *Chem. Eng. Sci.*, vol. 61, no. 13, pp. 4403–4416, 2006, doi: 10.1016/j.ces.2006.01.039.
- [12] H. B. Ma, C. Wilson, Q. Yu, K. Park, U. S. Choi, and M. Tirumala, “An experimental investigation of heat transport capability in a nanofluid oscillating heat pipe,” *J. Heat*

- Transfer*, vol. 128, no. 11, pp. 1213–1216, 2006, doi: 10.1115/1.2352789.
- [13] T. J. Rennie and V. G. S. Raghavan, “Experimental studies of a double-pipe helical heat exchanger,” *Exp. Therm. Fluid Sci.*, vol. 29, no. 8, pp. 919–924, 2005, doi: 10.1016/j.expthermflusci.2005.02.001.
- [14] M. Shafahi, V. Bianco, K. Vafai, and O. Manca, “An investigation of the thermal performance of cylindrical heat pipes using nanofluids,” *Int. J. Heat Mass Transf.*, vol. 53, no. 1–3, pp. 376–383, 2010, doi: 10.1016/j.ijheatmasstransfer.2009.09.019.
- [15] Z. Wu, L. Wang, and B. Sundén, “Pressure drop and convective heat transfer of water and nanofluids in a double-pipe helical heat exchanger,” *Appl. Therm. Eng.*, vol. 60, no. 1–2, pp. 266–274, 2013, doi: 10.1016/j.applthermaleng.2013.06.051.
- [16] W. Xu, S. Wang, G. Liu, Q. Zhang, M. Hassan, and H. Lu, “Experimental and numerical investigation on heat transfer of Therminol heat transfer fluid in an internally four-head ribbed tube,” *Int. J. Therm. Sci.*, vol. 116, pp. 32–44, 2017, doi: 10.1016/j.ijthermalsci.2017.01.020.
- [17] B. Ghasemi and S. M. Aminossadati, “Brownian motion of nanoparticles in a triangular enclosure with natural convection,” *Int. J. Therm. Sci.*, vol. 49, no. 6, pp. 931–940, 2010, doi: 10.1016/j.ijthermalsci.2009.12.017.
- [18] R. S. Vajjha and D. K. Das, “Experimental determination of thermal conductivity of three nanofluids and development of new correlations,” *Int. J. Heat Mass Transf.*, vol. 52, no. 21–22, pp. 4675–4682, 2009, doi: 10.1016/j.ijheatmasstransfer.2009.06.027.
- [19] R. S. Vajjha, D. K. Das, and D. P. Kulkarni, “Development of new correlations for

- convective heat transfer and friction factor in turbulent regime for nanofluids,” *Int. J. Heat Mass Transf.*, vol. 53, no. 21–22, pp. 4607–4618, 2010, doi: 10.1016/j.ijheatmasstransfer.2010.06.032.
- [20] M. Corcione, “Heat transfer features of buoyancy-driven nanofluids inside rectangular enclosures differentially heated at the sidewalls,” *Int. J. Therm. Sci.*, vol. 49, no. 9, pp. 1536–1546, 2010, doi: 10.1016/j.ijthermalsci.2010.05.005.
- [21] H. Stevenson, “Laser Velocimetry and Particle Sizing . Edited by H . DOYLE,” vol. 103, 1981.
- [22] F. Kreith *et al.*, *Heat and mass transfer*. 2004.
- [23] R. L. Manlapaz and S. W. Churchill, “Fully developed laminar flow in a helically coiled tube of finite pitch,” *Chem. Eng. Commun.*, vol. 7, no. 1–3, pp. 57–78, 1980, doi: 10.1080/00986448008912549.